Planta (2009) 229:427–445
DOI 10.1007/s00425-008-0841-y

ORIGINAL ARTICLE

Metabolomic and genetic analyses of flavonol synthesis in *Arabidopsis thaliana* support the in vivo involvement of leucoanthocyanidin dioxygenase

Ralf Stracke · Ric C. H. De Vos · Lutz Bartelniewoehner · Hirofumi Ishihara · Martin Sagasser · Stefan Martens · Bernd Weisshaar

Received: 19 August 2008 / Accepted: 10 October 2008 / Published online: 8 November 2008

Abstract Flavonol synthase (FLS) (EC-number 1.14.11.23), the enzyme that catalyses the conversion of flavonols into dihydroflavonols, is part of the flavonoid biosynthesis pathway. In *Arabidopsis thaliana*, this activity is thought to be encoded by several loci. In addition to the *FLAVONOL SYNTHASE1 (FLS1)* locus that has been confirmed by enzyme activity assays, loci displaying similarity of the deduced amino acid sequences to FLS1 have been identified. We studied the putative *A. thaliana FLS* gene family using a combination of genetic and metabolite analysis approaches. Although several of the *FLS* gene family members are expressed, only *FLS1* appeared to influence flavonoid biosynthesis. Seedlings of an *A. thaliana fls1* null mutant (*fls1-2*) show enhanced anthocyanin levels, drastic reduction in flavonol glycoside content and concomitant accumulation of glycosylated forms of dihydroflavonols, the substrate of the FLS reaction. By using a *leucoanthocyanidin dioxygenase (ldox) fls1-2* double mutant, we present evidence that the remaining flavonol glycosides found in the *fls1-2* mutant are synthesized in planta by the FLS-like side activity of the LDOX enzyme.

Keywords *Arabidopsis* · Dihydroflavonol · Flavonoid biosynthesis · Flavonol synthase · Leucoanthocyanidin dioxygenase

Abbreviations

ANR	Anthocyanidin reductase
CHS	Chalcone synthase
CHI	Chalcone isomerase
DFR	Dihydroflavonol 4-reductase
DHF	Dihydroflavonol
DPBA	Diphenylboric acid 2-aminoethylester
EBG	Early biosynthetic gene
ESI	Electro spray ionization
F3H	Flavanone 3β-hydroxylase
F3′H	Flavonoid 3′-hydroxylase
FLS	Flavonol synthase
GT	Glycosyltransferase
GUS	β-Glucuronidase
GUS′	Standardized specific β-glucuronidase activity
HPLC	High performance liquid chromatography
HPTLC	High performance thin layer chromatography
LBG	Late biosynthetic gene
LC	Liquid chromatography
LUC	Luciferase
LDOX	Leucoanthocyanidin dioxygenase
MS	Mass spectrometry
MU	4-Methylumbelliferone

Nucleotide sequence database accession numbers: GenBank accession EU287457 and EU287459.

Electronic supplementary material The online version of this article (doi:10.1007/s00425-008-0841-y) contains supplementary material, which is available to authorized users.

R. Stracke (✉) · L. Bartelniewoehner · H. Ishihara · M. Sagasser · B. Weisshaar
Chair of Genome Research, Bielefeld University, 33594 Bielefeld, Germany
e-mail: ralf.stracke@uni-bielefeld.de

R. C. H. De Vos
Plant Research International, 6700 AA Wageningen, The Netherlands

R. C. H. De Vos
Centre for Biosystems Genomics, 6700 AB Wageningen, The Netherlands

S. Martens
Institute of Pharmaceutical Biology, Philipps University, 35037 Marburg, Germany

PDA	Photo-diode array
QTOF	Quadrupole-time-of-flight
3GT	Anthocyanidin 3-O-glycosyltransferase

Introduction

Flavonoids are widely distributed in the plant kingdom, and they fulfil diverse vital functions. Besides the most visible role of flavonoids, the formation of red and purple anthocyanin pigments, flavonoid compounds serve as signals for pollinators and other organisms, participate in plant hormone signalling, facilitate pollen-tube growth (reproduction), protect plants from UV radiation, and function as phytoalexins and allelopathic compounds (Harborne and Williams 2000; Winkel-Shirley 2001). Flavonoids also play a role in human nutrition and have pharmaceutical potential (summarized in Harborne and Williams 2000; Ross and Kasum 2002). Recent metabolic engineering efforts to up-regulate flavonol biosynthesis in different plant species (Bovy et al. 2002; Reddy et al. 2007) and in *Escherichia coli* (Leonard et al. 2006) demonstrate that the understanding of flavonol synthesis is of particular interest.

Flavonoid biosynthesis (Fig. 1) proceeds from 4-coumaroyl- and malonyl-CoAs to naringenin chalcone, which is stereospecifically converted into the flavanone (2*S*)-naringenin (Heller and Forkmann 1994). Naringenin can be oxidized by flavone synthase (FNS) to form the flavone apigenin (Martens and Forkmann 1999; Martens et al. 2001) or hydroxylated by flavanone 3β-hydroxylase (F3H or FHT) to form a dihydroflavonol (3-hydroxyflavanone or flavanonol). Dihydroflavonols might subsequently be reduced to leucoanthocyanidins by the activity of dihydroflavonol 4-reductase (DFR) along the branch leading to flavan-3-ols, proanthocyanidins and anthocyanidins (Fig. 1). Alternatively, the oxidation of the dihydroflavonol to a flavonol is catalysed by flavonol synthase (FLS).

Flavonol synthase had been reported initially from irradiated parsley cells and has been classified as a dioxygenase essential requiring 2-oxoglutarate and Fe^{II} (ascorbate near essential) for optimal activity (Britsch et al. 1981). FLS activity was subsequently detected in flower tissues of *Matthiola incana* (Spribille and Forkmann 1984), *Petunia hybrida* (Forkmann et al. 1986) and *Dianthus caryophyllus* (Forkmann 1991). The first FLS cDNA was cloned from *P. hybrida* and identified by functional expression in yeast (Holton et al. 1993). Transformation of petunia or tobacco with antisense *FLS* intensified red flower pigmentation (Holton et al. 1993). Further FLS cDNAs were isolated from *Arabidopsis thaliana* (Pelletier et al. 1997; Wisman et al. 1998), *Eustoma grandiflorum*, *Solanum tuberosum* (van Eldik et al. 1997), *Malus domestica* and *Matthiola incana* (database submissions AF119095 and AF001391). The *A. thaliana* enzyme was expressed in and purified from *Escherichia coli*, and it was shown to catalyse in vitro the formation of quercetin and kaempferol from the corresponding dihydroflavonol precursors (Wisman et al. 1998), accepting (2*R*,3*S*)-dihydrokaempferol as the most effective substrate (Prescott et al. 2002). Unexpectedly, (2*S*)-flavanones were also accepted as substrates and converted almost completely to the respective flavonols via dihydroflavonols (Prescott et al. 2002).

Kinetic parameters and amino acid residues important for enzyme activity were reported for the *Citrus unshiu* (Lukacin et al. 2003) and *A. thaliana* (Chua et al. 2008) FLS enzymes. Another FLS site activity was reported from *A. thaliana* leucoanthocyanidin dioxygenase (LDOX; synonym: anthocyanidin synthase): the recombinant enzyme primarily exhibited in vitro FLS activity with negligible LDOX activity (Welford et al. 2001; Turnbull et al. 2003, 2004).

Flavanol synthase is the only enzyme of the central flavonoid pathway thought to be encoded by multiple genes in *A. thaliana* (Pelletier et al. 1997). Beside the characterized gene *FLS1* (At5g08640), five putative *FLS* genes (*FLS2–FLS6*) have been identified in the *A. thaliana* genome (Fig. 2, Supplementary Figure 1). The role of the FLS homologs in *A. thaliana* is still unknown. Two hypotheses could explain the existence of this putative redundancy: (1) FLS isoforms are varying in substrate specificities with preference for a given dihydroflavonol subclass; this is supported by the report of a dominance for the synthesis of kaempferol for FLS1 (Wisman et al. 1998) as well as the predominant accumulation of divergent flavonols in different tissues, (2) FLS isoforms are tissue-specific and are differentially expressed during development and in response to environmental signals; this is supported by tissue specific expression of the *FLS* genes as deduced from publicly available microarray data.

When we initiated our study, the aim was to characterize the *FLS* gene family in *A. thaliana* using genetic and biochemical methods, to test the hypothesis that different *FLS* genes are used to mediate differential synthesis of flavonols in different tissues or cell types. Our approach was to analyse the responsiveness of *FLS* gene family members to regulatory transcription factors being essential for functional FLS activity in the seedling, and to use *fls* knock-out mutants for this purpose, analysing the association of mutant phenotypes with flavonoid metabolism. We identified and characterized insertional null mutants for all six family members. Targeted metabolite analyses indicate that *fls2–fls6* mutant seedlings seem to have no defect in flavonol accumulation. The *fls1* mutant shows a drastic reduction in flavonol glycoside content, higher levels of anthocyanins and the concomitant accumulation of glycosylated forms of dihydroflavonols, the substrate of the FLS

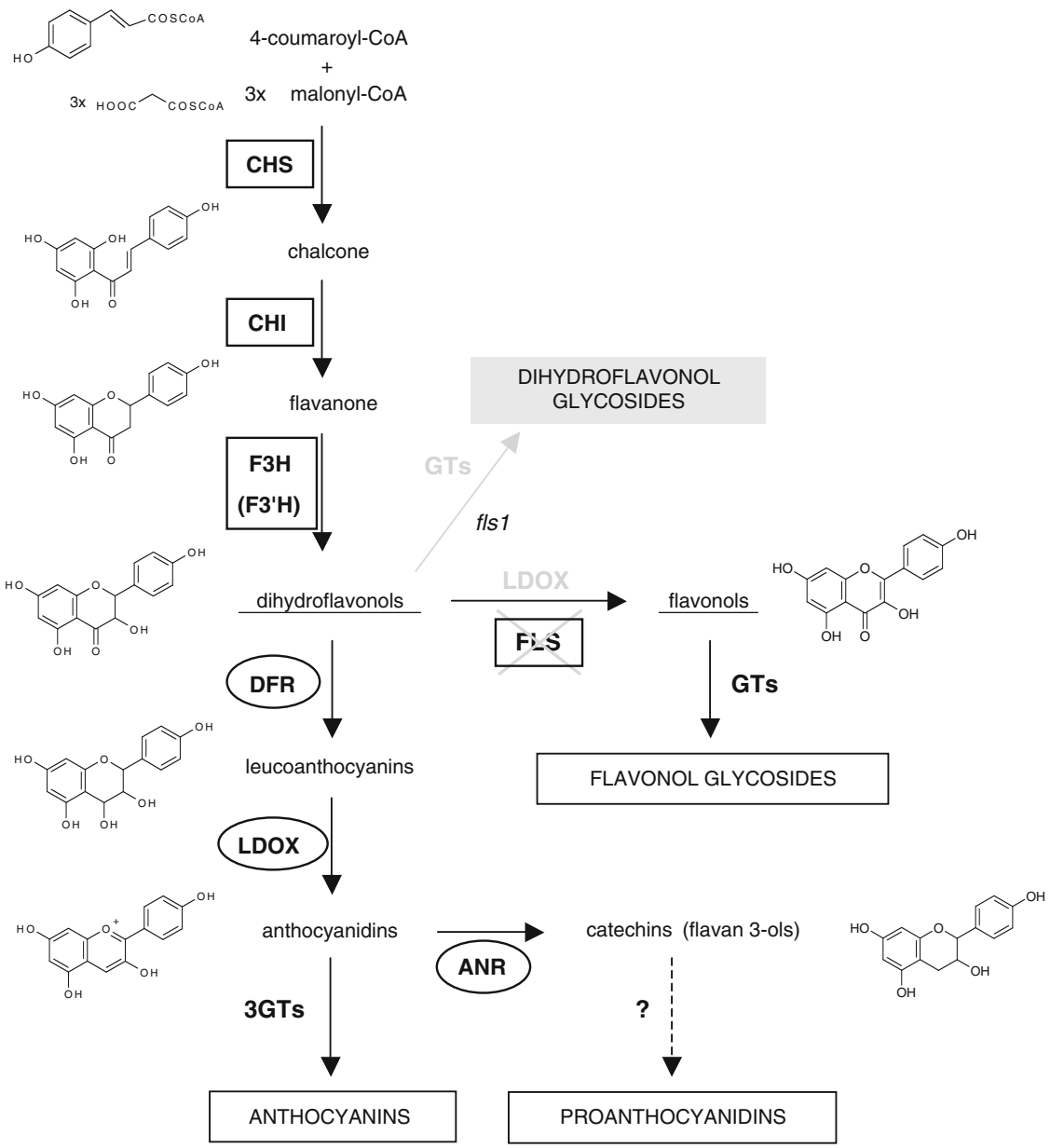

Fig. 1 Simplified, schematic representation of flavonoid biosynthesis in *A. thaliana*. To make this figure more comprehensive, results from this paper have been included. Enzymes are indicated by *bold, capital letters*. Based on the positions of individual enzymes in the pathway and the timing of activation of the respective genes, flavonoid biosynthesis in dicotyledonous plants has been subdivided into early (EGB) and late (LGB) biosynthetic groups of genes (Martin et al. 1991; Kubasek et al. 1992; Quattrocchio et al. 1993). As schematically depicted, EBGs comprise the steps from phenylpropanoid precursors to flavonols, whereas LBGs are involved in the formation of anthocyanins and proanthocyanidins. EBGs are *boxed*; LGBs are *circled*. Abbreviations are as follows: *ANR* anthocyanidin reductase, *CHS* chalcone synthase, *CHI* chalcone isomerase, *DFR* dihydroflavonol 4-reductase, *DHF* dihydroflavonol, *F3H* flavanone 3β-hydroxylase, *F3′H* flavonoid 3′-hydroxylase, *FLS* flavonol synthase, *GTs* glycosyltransferases, *LDOX* leucoanthocyanidin dioxygenase, *3GTs* anthocyanidin 3-*O*-glycosyltransferases. The *grey box* indicates metabolites accumulating in the *fls1* mutant. The pathway leading to the formation of isorhamnetin (4′-methoxy quercetin) is not illustrated

reaction. We further present evidence that the remaining flavonol glycosides found in the *fls1* mutant are synthesized by the in planta FLS-like site activity of LDOX. During our study, Owens et al. (2008a) provided evidence that FLS1 appears to be the only member of this group that influences flavonoid levels. Their findings will be discussed in relation to our data.

Materials and methods

Standard molecular biology methods

Essentially, standard molecular biology techniques were carried out. DNA sequencing was performed using Big-Dye terminator chemistry on 3730 sequencers (Applied

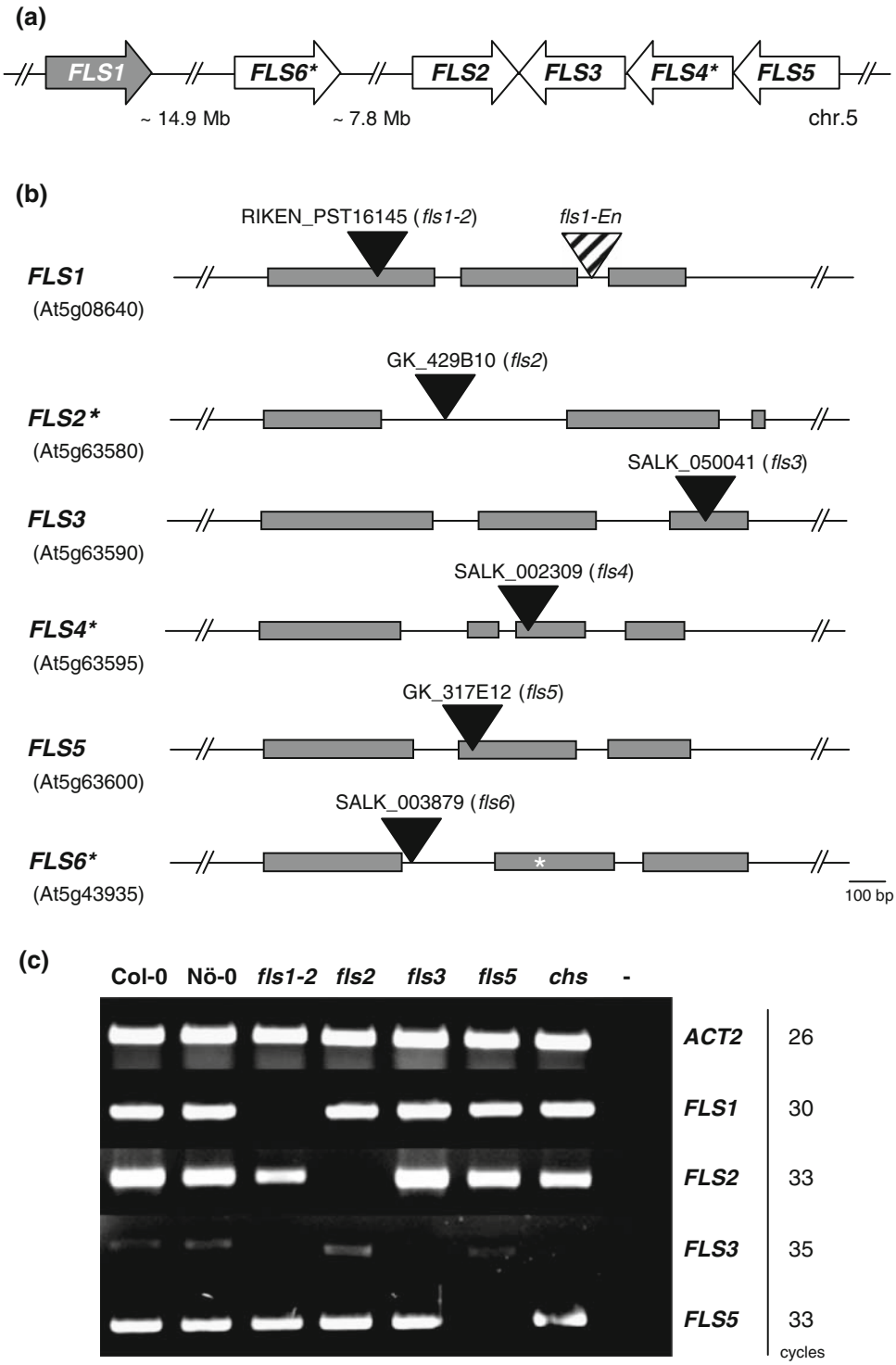

Fig. 2 *fls* mutant alleles. **a** Genomic arrangement of *FLS* genes on *A. thaliana* chromosome 5. The genes *FLS2–FLS5* are consecutively arranged. **b** Structure of *FLS* wildtype and mutant alleles. The exon/intron structure is depicted, where *grey boxes* indicate coding- and *thin black lines* symbolize non-coding regions. Positions of T-DNA insertions are given as *black triangles*; transposon insertion in *fls1-En* is marked as *striped triangle*. Putative pseudogenes are marked with a *black asterisk*. The position of the premature stop codon in *FLS6* is indicated by a *white asterisk*. **c** Results from RT-PCR showing the expression of *ACT2, FLS1, FLS2, FLS3* and *FLS5* in 5-day-old *A. thaliana* wildtype and mutant seedlings, indicating that *fls1–2, fls2, fls3* and *fls5* are null alleles. Numbers of amplification cycles are given at the *right*

Biosystems; Foster City, CA, USA). Oligonucleotides were purchased from Metabion (Martinsried, Germany) or Invitrogen (Paisley, UK).

Plant material

Mutant alleles were identified from the SIGnAL/SALK, GABI-Kat and RIKEN populations. Seed stocks were obtained from the Nottingham Arabidopsis Stock Centre (NASC), GABI-Kat and RIKEN, respectively. The mutants are described in Fig. 2b. Sequences of newly characterized alleles were submitted to GenBank (accession numbers: EU287457 and EU287459). The homozygous *ldox fls1-2* double mutant was produced by crossing and the progeny was analysed using PCR markers that distinguish between mutant and wildtype alleles (see below).

Growth conditions

Surface-sterilized *A. thaliana* seeds were sown on 0.5 MS with 1.5% sucrose on 0.8% agar plates, kept for 2 days at 4°C in the dark, and then transferred to a phytochamber with 16 h light illumination per day at 22°C. Seedlings were harvested at the fifth day after germination (5 day old; i.e. 6 days after transfer into the light).

RT-PCR

RNA was isolated using the RNeasy® Plant Mini Kit (Qiagen, Hilden, Germany) following the manufacturers instructions. cDNA was synthesized from 2 µg total RNA in a 20 µl volume using an oligo dT primer and SuperscriptII RT (Invitrogen) at 42°C in 1 h. One microlitre of resulting cDNA was used as template in the subsequent PCR: 25 µl volume containing 20 mM Tris–HCl (pH 8.4), 50 mM KCl, 1.5 mM $MgCl_2$, 0.2 mM each dNTP, 0.2 µM each primer and 1.5 U *Taq* DNA polymerase (Invitrogen) using the cycling protocol: 3 min, 95°C—20 s, 94°C; 20 s, 58°C and 90 s, 72°C—2 min, 72°C. Nine microlitres of the amplification products were analysed by electrophoresis and visualized by ethidium bromide staining on a 1% agarose gel. The following primers were used: RS469 (5′-TC CGCTCTTTCTTTCCAAGCTCAT-3′) and RS470 (5′-TC CAGCACAATACCGGTTGTACG-3′) for detection of *ACT2* transcripts, RS652 (5′-GTTCAAGCGCATGTGCGACA AGTCG-3′) and CHS-RP (5′-TCTCTCCGACAGATGT GTCAGG-3′) for *CHS*, L80 (5′-CTTTGACTG AGCTAG CCGGA-3′) L81 (5′-GAGGGTGAGATCAGGCTGAG-3′) for *F3H*, B74 (5′-GGCTAGTGATGCGATTACT-3′) and B75 (5′-CAACACCTTCAAACGTTGA-3′) for *DFR*, S251 (5′-AGACCATGGTTGCGGTTGAAAGAGTTG-3′) and S252 (5′-ATCATTTTTCTCGGATACCAATTC CTC-3′) for *LDOX*, RS873 (5′-CTTCTCTTTCTTCAACA CCGCACA-3′) and RS874 (5′-GCTAATGTACGCCA CAGAACCAGA-3′) for *UGT78D2*, and RS877 (5′-CACG TTCTGGTGATACCGTTTCCA-3′) and RS878 (5′-GGC TTCCAAAACCGACGTATACGA-3′) for detection of *UGT89C1*. The *FLS* transcripts were detected with the following primers: FM147 (5′-CCGTCGTCGATCTAAGCG AT-3′) and FM53 (5′-CCTCCCATTACTCAACC TCAG-3′) for *FLS1*, RS626 (5′-ACAAGTTTGTACAAAAAAGCA GGCTCCATGGAAGTTGAGAGAGATCAACACATTT C-3′) and RS640 (5′-ACCACTTTGTACAAGAA AGCTGGGTTCTATGCAACACATTCTTGTACTTTC-3′) for *FLS2*, RS706 (5′-ATGGAGATGGAGAAAAACC AACACATTTC-3′) and RS737 (5′-TTTTTTTTATT CATGATCTCTTTTCTG-3′) for *FLS3*, RS632 (5′-GA TGAAGACTTCTTGGTGCGTGAGG-3′) and RS633 (5′-AACAACCACGGCGGAGTCGATATAG-3′) for *FLS5*. All RT-PCRs were done in two biological and two technical replicates. The presented pictures are representative.

Transfection experiments

Protoplast isolation and transfection experiments for detection of transient expression were performed as described by Mehrtens et al. (2005). In the cotransfection experiments, a total of 25 µg of premixed plasmid DNA was transfected, consisting of 10 µg of reporter plasmid, 1 µg of effector plasmid and 5 µg of the luciferase (LUC) standardization plasmid. Protoplast were incubated for 20 h at 26°C in the dark before LUC and GUS enzyme activities were measured. Specific GUS activity is given in pmol 4-methylumbelliferone per mg protein per minute. Standardized specific GUS activity (GUS′) was calculated by multiplication of the specific GUS activity value with a correction factor derived from the ratio of the specific LUC activity in the given sample to the mean specific LUC activity (describing the transformation efficiency) of a set of six complete experiments. The error bars indicate the standard deviation of the six GUS′ values for the respective construct. Reporter constructs for transfection experiments were generated by PCR using primers RS610 (5′-ATG AGAAGCTTGAATAATTCTTGTGTAGTGAGTTGA-3′, with *Hin*dIII site) and RS611 (5′-CAACTTCCATGGTG GTCGCTGGAAATAATGG-3′, with *Nco*I site in ATG start-codon) resulting in a 1,041-bp fragment for pro_{FLS2}, RS612 (5′-AACCGGATCCTATTAATTGAAGTTCAAA CAAA-3′, with *Bam*HI site) and RS613 (5′-CCATCTCC ATGGTTTTCAGTTTCACTCG-3′, with *Nco*I site in ATG start-codon) resulting in a 699-bp fragment for pro_{FLS3}, RS614 (5′-AAGTCGGATCCGGACAAATTGAGGATT TCTT-3′, with *Bam*HI site) and RS615 (5′-GACCTCC ATGGTTCTAATTTTTTTGTGATCAATC-3′, with *Nco*I site in ATG start-codon) giving a 830-bp fragment for pro_{FLS4}, RS616 (5′-TTGTTAACGTTACCATCAGTTTC ATAATAG-3′, with *Hin*dIII site) and RS617 (5′-TTCTT CCATGGCTTCATAGGTGTGAGAAGGA-3′, with *Nco*I site in ATG start-codon) resulting in a 786-bp fragment for pro_{FLS5}, and RS618 (5′-TATCTAAGCTTCAATTGCAAT TCATAATATGAG-3′, with *Hin*dIII site) and RS619 (5′-GACGTCCATGGTTGTTCACTCTCTCTTCTCCA-3′, with *Nco*I site in ATG start-codon) for pro_{FLS6} with a size of 1,199 bp. *Hin*dIII/*Nco*I or *Bam*HI/*Nco*I cut promoter fragments were cloned into pBT10-GUS (Sprenger-Haussels and Weisshaar 2000). The pro_{FLS1} reporter construct has been described previously (Mehrtens et al. 2005).

Crossing and genotyping of mutants

Genomic DNA for PCR analysis was isolated from rosette leaves using a slightly modified protocol described by

Edwards et al. (1991). PCR was carried out in a 25 µl volume using 0.3 µl *Taq* DNA polymerase (Invitrogen) and 2 µl genomic DNA. An amplicon of 1,303 bp was produced using the primers B078 (5′-TTCCCCTGTTTTTAAGTTTATTT-3′) and B079 (5′-AGAAAGACACAAACACATTATAAA-3′) detecting the *LDOX* wildtype allele. The *ldox* mutant allele (SALK028793) was detected using the primer combination B078 and RS630 (5′-GCGTGGACCGCTTGCTGCAACTCTCTCAGG-3′) resulting in a PCR product of about 900 bp. In case of *FLS1* the wildtype allele was traced by the primers RS647 (5′-TTACACATATCAACACGTACTTTA-3′) and UH9 (5′-CACTGAGATCTGTATGAGCCGGTACACC-3′), while the insertion allele was detected by the combination of primers RS645/Ds3-2a (5′-CCGGATCGTATCGGTTTTCG-3′) and UH9. In case of the wildtype allele a PCR product of about 1,000 bp was obtained, while the PCR product of the mutant allele was about 600 bp.

Methanolic extracts for HPTLC analysis

Methanolic extracts were produced from 20 to 150 mg plant material in 2 ml reaction tubes by addition of 0.4 ml 80% methanol and about 10–15 zirconia beads of 1 mm diameter (Roth, Karlsruhe, Germany). Samples were homogenized at maximum speed in a Ribolyser (Q-BIOgene, Carlsbad, CA, USA) at a setting of 6.5 m/s, three times for 45 s. Homogenized samples were incubated for 15 min at 70°C and centrifuged for 10 min at 15,700*g*. Supernatants were vacuum-dried in a SpeedVac at 60°C. The dried pellets were dissolved in 1 µl of 80% methanol per mg starting material for high performance thin layer chromatography (HPTLC).

High performance thin layer chromatography

High performance thin layer chromatography and DPBA-staining (diphenylborate 2-aminoethylester) were performed as described by Stracke et al. (2007). Two microlitres of methanolic extracts were spotted on 10 cm × 10 cm silica-60 HPTLC plates (Merck) used as stationary phase. Chromatography was carried out using a system of ethyl acetate, formic acid, acetic acid, water (100:26:12:12, by vol.) as mobile phase in a closed glass tank. Separated phenylpropanoid compounds were stained by spraying a 1% diphenylboric acid 2-aminoethylester (DPBA, also known as Naturstoffreagenz A; Roth 9920-1) solution in methanol (w/v), followed by spraying 5% methanolic PEG 4000 (w/v) solution. The stained chromatograms were examined under UV light (365 nm) and photographed. Anthocyanins could be detected by this method without staining and UV illumination.

Identification of re-extracted HPTLC spots

The extracted spots were redissolved in 75% MeOH and analysed by liquid chromatography coupled to high-resolution mass spectrometry (LC-PDA-QTOF-MS), to compare their retention times, adsorbance spectra and accurate masses with compounds from wildtype and mutant *A. thaliana* samples. In addition, the extracted spots were analysed by QTOF-MS/MS, to verify the proposed glycosides and aglycon structures.

Untargeted metabolomics of plant tissues

For each line, seedlings from independent Petri dishes were harvested, samples were ground in liquid nitrogen and 100 mg of each sample was weighed in Eppendorf tubes. Aqueous-methanolic extracts, reverse phase LC-PDA-QTOF-MS analyses and data-processing (unbiased mass peak extraction and alignment of data) using the software program *MetAlign* were performed as described by De Vos et al. (2007). After extraction and alignment of all mass signals with a signal-to-noise ration higher than 3, signals with intensities (peak height) lower than 100 ion counts per scan in all samples were discarded, leaving 4,818 signals. Subsequently, the so-called multivariate mass spectra reconstruction strategy (Tikunov et al. 2005) was used to cluster mass signals, including natural isotopes, adducts and in-source fragments, derived from the same compound. A correlation coefficient of 0.7 and retention window of 15 s were used as thresholds. This mass signal clustering revealed 221 clusters and 292 single mass signals. From each cluster, the parent ion was selected, based upon the fact that they normally represent the highest signal intensity within a cluster and by checking the mass spectra of the original chromatograms. Student's *t*-tests were performed to determine the significant differences between mutant and wildtype plants. Accurate masses of differential parent ions were calculated manually, taking into account the correct ion intensity range (Moco et al. 2006). Compounds were (putatively) identified by comparing the MotoDB (http://appliedbioinformatics.wur.nl/moto/; Moco et al. 2006), Dictionary of Natural Products (www.chemnetbase.com), KNApSAcK (http://kanaya.naist.jp/KNApSAcK) and/or ChemSpider (http://www.chemspider.com). Suggested elemental compositions and annotations were checked for the presence of corresponding in-source fragments in the mass clusters and for absorbance spectra in the original data files. In all cases of annotated flavonoids, the observed masses were within 5 ppm deviation from the calculated masses.

Results

The *FLS* gene family in *A. thaliana*

Since the (almost) complete genome sequence of *A. thaliana* has been published (TASP, 2000), five genes (*FLS2*, At5g63580; *FLS3*, At5g63590; *FLS4*, At5g63595; *FLS5*, At5g63600 and *FLS6*, At5g43935) have been identified, showing high similarity to FLSs from *A. thaliana* (FLS1) and other species (Supplementary Figure 1). Their polypeptide sequences share 56–75% similarity and 45–64% identity with FLS1 (FLS2, 56% similarity/45% identity; FLS3, 75%/64%; FLS4, 61%/48%; FLS5, 69%/52%; FLS6, 74%/61%). However, it is unclear whether these *FLS* genes are encoding functional FLSs. *FLS6* appears to be a pseudogene because it contains a premature stop codon in the second exon (Fig. 2b), and no corresponding ESTs have so far been identified. Additionally, we failed to amplify corresponding transcripts by RT-PCR using a variety of cDNA templates (data not shown). *FLS4* may also be non-functional as analysis of a full-length cDNA clone (RAFL14–71-I18) indicates that, in contrast to the other *FLS* genes, it contains an additional intron, truncating the coding region. Expression of the remaining genes *FLS2*, *FLS3*, *FLS5* in *A. thaliana* could be shown by RT-PCR in developing seedlings, with comparable expression levels for *FLS1*, *FLS2* and *FLS5* and low levels in case of *FLS3* (Fig. 2c). Although the *FLS2* gene is transcribed, it is fairly unlikely that the resulting protein has FLS activity. The deduced polypeptide from the *FLS2* transcript is missing the C-terminal protein part (Supplementary Figure 1), including the last histidine residue of the HxD…H motiv involved in 2-oxoglutarate binding (Britsch et al. 1993; Roach et al. 1995; Lukacin and Britsch 1997) as well as the amino acid residues involved in iron binding (Myllylä et al. 1992; Britsch et al. 1993; Lukacin and Britsch 1997; Clifton et al. 2006). Taken together, these results indicate that only *FLS1*, *FLS3* and *FLS5* encode full-length proteins.

Additional in silico expression analyses using the *A. thaliana* "electronic fluorescent protein" (eFP) browser (http://bbc.botany.utoronto.ca/efp/cgi-bin/efpWeb.cgi) indicated that *FLS1* is expressed in reproductive structures (inflorescence, siliques, seeds), stem and the shoot apex ($signal_{max}$ = 2090). *FLS2* is expressed in stems and developing seeds (stages 3–5) ($signal_{max}$ = 213). *FLS3* is expressed in stages 7–8 of seed development ($signal_{max}$ = 241), while *FLS5* seems to be exclusively expressed in roots, predominantly in the epidermal layer and the stele ($signal_{max}$ = 1257). These results indicate a differential expression of the *FLS* genes.

Regulation of *FLS* gene promoters by R2R3-MYB PFG factors

The expression of flavonoid biosynthesis enzyme genes is mainly regulated by the activity of transcription factors of R2R3-MYB, BHLH and BZIP type (overview in Quattrocchio et al. 2006). In the *A. thaliana FLS1* promoter two *cis*-active elements have been described: a MYB-recognition element (MRE), bound by R2R3-MYB proteins and an ACGT-containing element (ACE) (Hartmann et al. 2005). Regions with sequence similarities to ACEs (ACSs) and R-recognition elements (recognized by BHLH factors) are found in promoter regions of all *FLS* genes, while MRE-like sequences are found in 5′-upstream regions of *FLS2, FLS4, FLS5* and *FLS6* (Fig. 3a).

The R2R3-MYB transcription factors—production of flavonol glycoside1–3 (PFG1–PFG3) have been described as flavonol-specific regulators of flavonoid biosynthesis (Mehrtens et al. 2005; Stracke et al. 2007), activating the transcription of *FLS1* in vivo. The regulatory potential of these three proteins on *FLS* promoters was tested in transient co-transfection experiments using *A. thaliana* At7 protoplasts (Fig. 3b). *FLS* gene promoters were fused to the *uidA* ORF (GUS), and standardized β-glucuronidase activity (GUS′) was taken as a measure for target promoter activity. We assayed the *FLS* promoters for their responsiveness to PFG1, PFG2 and PFG3, using the *FLS1* promoter (pro_{FLS1}) as a control. In contrast to pro_{FLS1}, the other *FLS* gene promoters were not responsive to any of the three R2R3-MYB transcription factors. This indicates that the *FLS2–FLS6* promoters are not targets of the PFG factors.

Identification and characterization of *FLS* gene mutants

To examine the function of *FLS1–FLS6* in planta, we isolated *A. thaliana* plants carrying mutant alleles of these genes by reverse genetics. For *FLS2–6*, mutant lines with T-DNA insertions in coding or intronic regions (Fig. 2b) were identified from the GABI-Kat and SALK populations, all in Col-0 background. The *fls1-En* line described previously (Wisman et al. 1998) carries an active *En-1* element in the second intron of *FLS1* and often shows phenotypic reversion to wild type caused by excision of the *En-1* transposon from the locus. A stable *FLS1* mutant line was identified from the RIKEN population: line PST16145 with a T-DNA insertion in the first exon (designated *fls1-2*; Nö-0 genetic background; Fig. 2b). Results from RT-PCR indicate that *fls1-2, fls2, fls3* and *fls5* are null alleles (Fig. 2c).

Since the sequence-related *FLS* gene products could have similar functional activity, we constructed double-mutants of *fls1-2* with single *fls2–fls6* gene mutants for our analyses. The consecutive genomic arrangement of the *FLS*

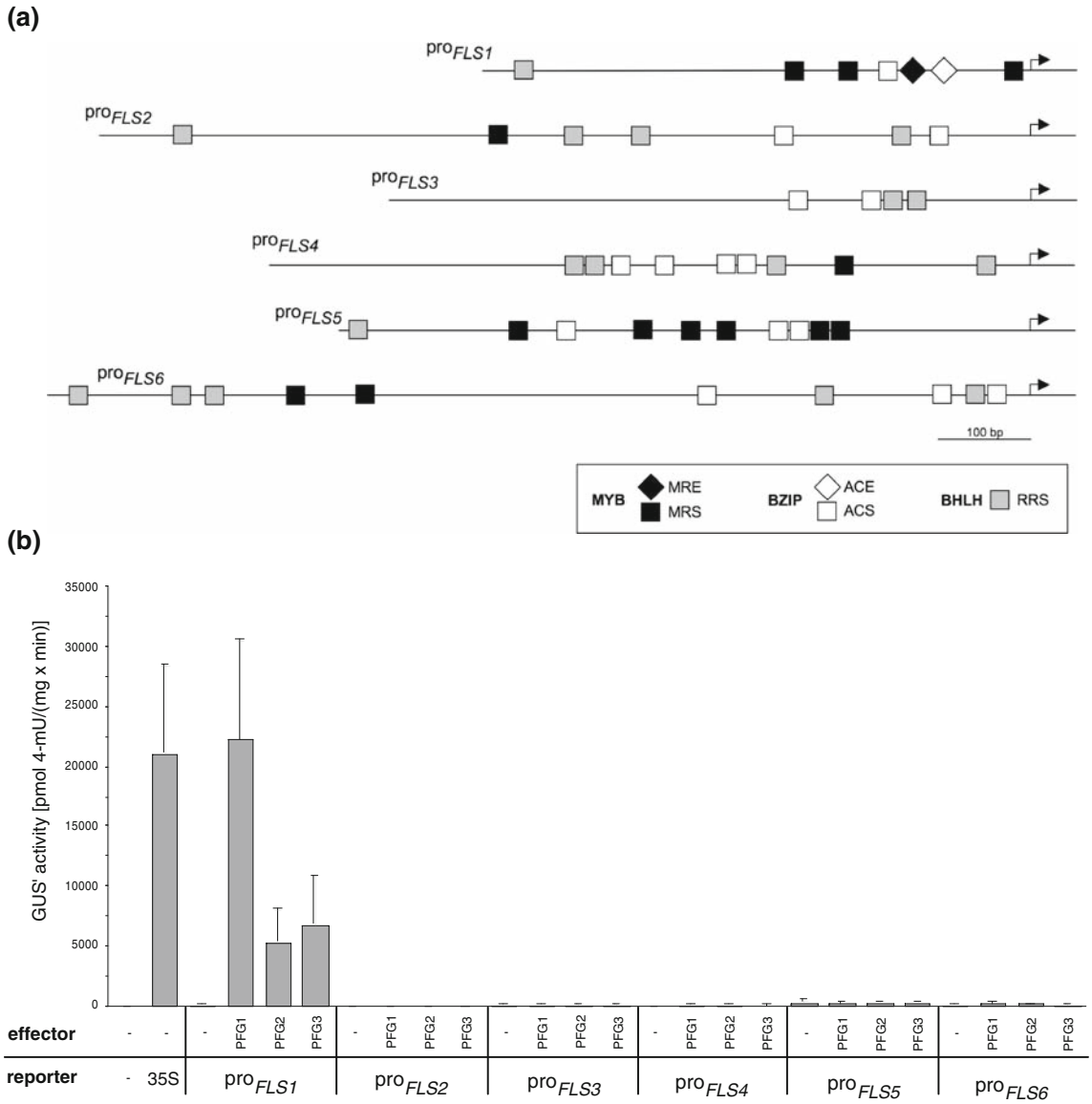

Fig. 3 *A. thaliana FLS* family promoter analysis. **a** Positions of (putative) MYB, BZIP and BHLH transcription factor binding sites in the *A. thaliana FLS* family promoters. *Diamonds* indicate proven MYB recognition elements (MREs) and proven ACGT containing elements (ACEs) in the *FLS1* promoter (Hartmann et al. 2005). *Squares* label promoter regions with sequence similarities to known transcription factor binding elements: MRS (MRE-like sequence), ACS (ACE-like sequence) and RRS (R-recognition element-like sequence). The *bent arrow* marks the start site of translation. **b** Transient co-transfection analysis of target gene specificities in *A. thaliana* protoplasts. GUS-fused *FLS* promoter fragments (reporters) were assayed for their responsiveness to the effectors PFG1-3 by co-transfection experiments in At7 protoplasts. The figure shows standardized GUS′ activity resulting from the influence of tested effector proteins on different reporters. The mean value of luciferase activity, used for standardization, was 3175 RLU (relative luciferase units) µg protein^{-1} s^{-1} (see Sect."Materials and methods")

genes (Fig. 2a) hampered the generation of other multiple *fls* mutants. Neither of the double mutants did show any apparent visible difference in comparison to wildtype plants when grown under greenhouse conditions.

Flavonol accumulation in mutant seedlings

Accumulation of flavonols in the mutant seedlings was analysed in a targeted metabolomic approach applying HPTLC (Fig. 4a, b). Phenylpropanoid compounds were extracted from wildtype, *fls* mutants and from a *chalcone synthase/transparent testa4* (*chs/tt4*) mutant that completely lacks flavonoids. In extracts of wildtype seedlings, kaempferol glycosides (green fluorescence) and quercetin glycosides (orange fluorescence) were clearly detectable after DPBA staining and UV-illumination. A notable difference in the flavonol glycoside composition between the Col-0 and the Nö-0 accession was observed (asterisk in Fig. 4a). The

chemical nature of the respective compounds was determined by a successive combination of HPLC-photo diode array analyses and electro spray ionization/accurate mass spectroscopy followed by gas chromatography-mass spectroscopy for sugar analysis: Q* was identified as quercetin-[(glycosyl) glucoside]-rhamnoside and K* as kaempferol-[(glycosyl) glucoside]-rhamnoside [data not shown; the difference detected between Col-0 and Nö-0 has been described recently by Keurentjes et al. (2006)]. The flavonol glycoside patterns of *fls2–fls6* single mutants were similar to that observed in the corresponding Col-0 wildtype. In contrast, quite different patterns were found in the *fls1-2* mutant that seemed to lack all flavonol glycoside spots observed in the corresponding Nö-0 wildtype. Moreover, at least three new spots (1 to 3, Fig. 4a) were detected.

The *fls1*-specific compounds were re-extracted from the plates after HPTLC separation and analysed by accurate mass LC-PDA-QTOF-MS and MS/MS. This lead to the identification of the three spots as dihydroflavonol hexosides (Fig. 4c): Compound 1 could be identified as dihydroquercetin-hexoside, compound 2 as dihydrokaempferol-hexoside and compound 3 as dihydroquercetin-deoxyhexoside.

Anthocyanin accumulation in mutant seedlings

To analyse if changes in FLS activity may affect other flavonoids, we analysed the formation of anthocyanins in the seedling. Anthocyanins are present in Col-0 and Nö-0 wildtype seedlings, but are absent from the *ldox/tt18* mutant (Fig. 5). Purple anthocyanin pigments were clearly detectable in *fls1-2* seedlings, demonstrating that DFR and LDOX are active in this mutant. The level to which anthocyanins accumulate in the *fls1-2* mutant is reproducibly much higher than in the wildtype, indicating that precursors usually channelled to flavonols are used to build anthocyanins. In contrast, *fls2–fls6* mutant seedlings do not reveal any significant change in quality or quantity of anthocyanin accumulation (data not shown).

Metabolic analysis of *fls1-2* mutant seedlings

To assess the metabolic variation between the *A. thaliana* the *fls1-2* mutant and the corresponding wildtype (Nö-0) in a more comprehensive manner, we performed LC-PDA-QTOF-MS-based untargeted fingerprinting of acidified aqueous methanol extracts from 5-day-old seedlings. This allowed the detection of mostly glycosylated derivatives of phenolic acids, flavonoids, alkaloids and other small molecules. All mass signals with a signal-to-noise ratio ≥ 3 and signal intensities ≥ 100 ion counts per scan in all samples ($n = 3$) were automatically extracted and aligned using *MetAlign* software resulting in a data matrix of 4,818 mass signals (not metabolites). We observed considerable quantitative and qualitative variation in the mass profiles. After clustering of mass signals, from each cluster the parent ion was selected, based upon the fact that they normally represent the highest signal intensity within a cluster and by checking the mass spectra of the original chromatograms. Identification of the differential mass signals, based on accurate mass, MS/MS fragmentation patterns, PDA (UV/Vis)-signals and QTOF-MS, indicated many flavonol glycoside derivatives being significantly higher in wildtype, whereas several glycosides of dihydroflavonols were higher in the *fls1-2* mutant (Table 1). Various flavonol glycosides of kaempferol-, quercetin-, methyl-quercetin- (isorhamnetin-) and methyl-kaempferol-type show significant reduction in the *fls1-2* mutant seedlings, with a kaempferol-hexoside-dideoxyhexoside, a kaempferol-hexoside-deoxyhexoside and a kaempferol-dideoxyhexoside being the most differential ones. The dihydroflavonol derivatives accumulating in the *fls1-2* mutant have dihydroquercetin-, dihydrokaempferol- and methyl-dihydroquercetin-aglycones. The most differential compounds which are higher in the *fls1-2* mutant are a dihydroquercetin-deoxyhexoside and two dihydroquercetin-deoxyhexosides, fitting well to the identified metabolites from the HPTLC re-extracts (Fig. 4). Additional, six unknown flavonoids and an eriodictyol-deoxyhexoside were found to be differential accumulating between Nö-0 and *fls1-2*.

Analysis of *ldox fls1-2* double mutant

Flavanol synthase and LDOX are 2-oxoglutarate-/Fe^{II}-dependent dioxygenases and have been shown to have overlapping substrate and product selectivities in vitro (Martens et al. 2003; Turnbull et al. 2004). Recombinant LDOX was in vitro shown to form predominantly quercetin from *cis*- and *trans*-dihydroquercetin with cyanidin as minor product. To test the possibility that the observed remaining FLS catalytic activity in the *fls1-2* mutant is due to LDOX activity, the respective double mutant was generated. Using HPTLC, no difference was detected between the *ldox fls1-2* double mutant and the *fls1-2* single mutant (data not shown). Subsequently, the various mutants and wildtypes were screened for the presence of selected flavonol glycosides and dihydroxyflavonol glycosides using a very sensitive LC-PDA-QTOF-MS/MS system.

Relative accumulation data of two selected flavonol glycosides and two dihydroxyflavonol glycosides are given in Fig. 6a. Data for a sinapoyl-glucoside is given as unaffected compound control between the analysed genotypes, showing that equal amounts of seedlings were used in the analysis. A clear reduction of flavonol glycosides (kaempferol-hexoside-deoxyhexoside, RT 23,26 *m/z* 593; quercetin-dideoxyhexoside, RT 23,55 *m/z* 755) accumulation was

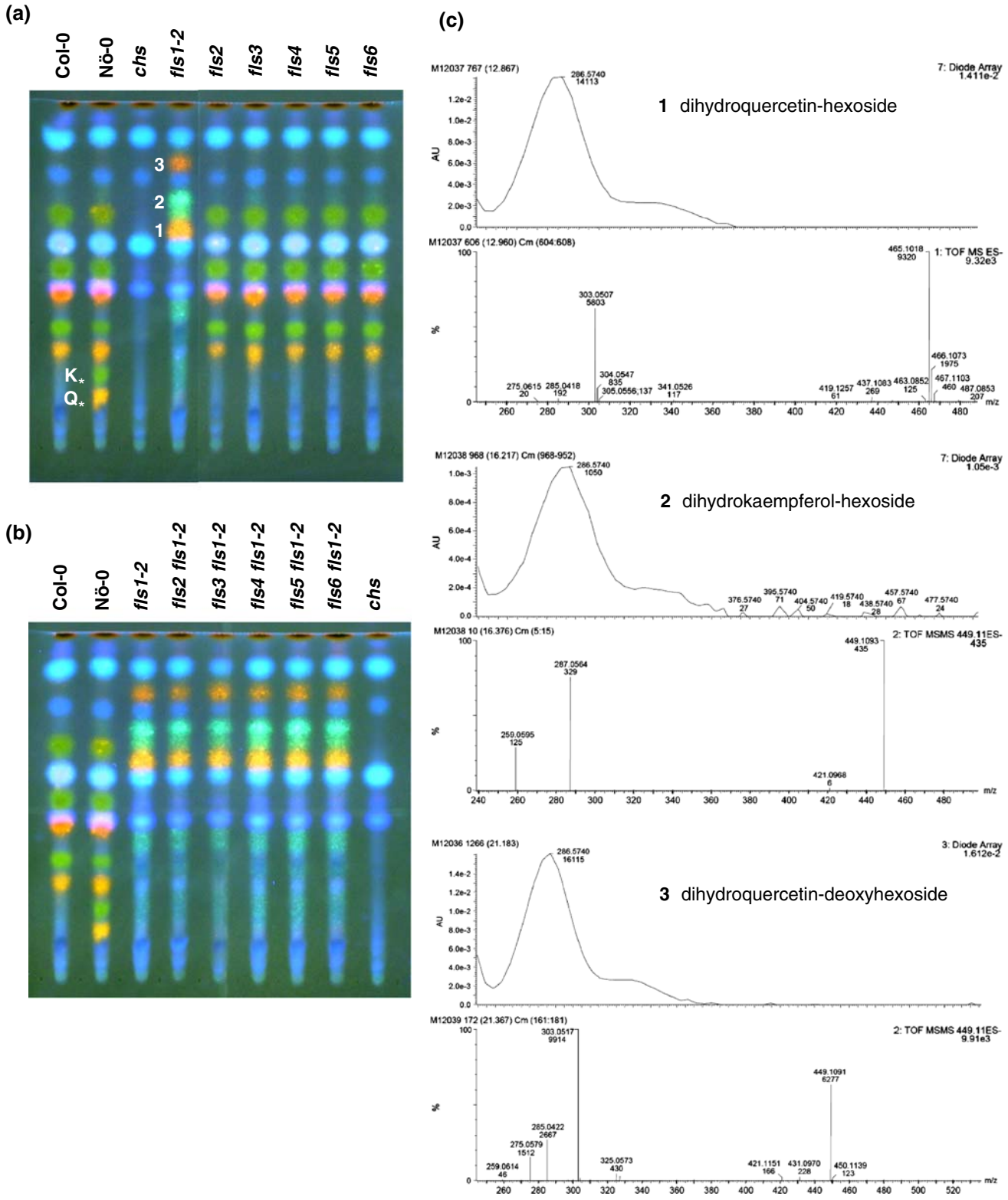

found in the *ldox fls1-2* double mutant compared to the *fls1-2* single mutant. Surprisingly, a comparison to the flavonoid-deficient *chs* mutant indicated that there are still very low but detectable levels of flavonol glycosides in the *ldox fls1-2* mutant. Since these metabolites are not detectable with PDA or UV detectors in the double mutant (data not shown), we assume that the levels of flavonol glycosides are less than 0.5 ppm (0.00005%) from the wildtype. The same holds for dihydroflavonol glycosides in the wildtype, where very low levels could be detected by

◀ **Fig. 4** Metabolic analysis of *fls* mutant seedlings. **a**, **b** Representative result of methanolic seedlings extracts separated by HPTLC on silica gel-60 plates followed by DPBA staining and UV-illumination. Colourkey: *green* kaempferol derivative, *orange* quercetin derivative, *faint blue* sinapate derivative, *pink* overlapping quercetin and sinapate derivatives, *dark red* chlorophyll. **a** Representative HPTLC of wildtype and single mutant seedlings. *Numbers* indicate spots exclusively found in the *fls1-2* mutant; these compounds have been re-extracted from the plates for analyses of their chemical nature leading to the identification of glycosylated dihydroflavonols (see **c**). *Letters with asterisk* indicate flavonol tri-glycosides found in the Nö-0, but not in the Col-0 background. **b** Representative HPTLC of *fls fls1-2* double-mutant seedlings. **c** Structure identification for compounds from re-extracted HPTLC spots. Extracted spots were redissolved in 75% MeOH and analysed by LC-PDA-QTOF-MS/MS. Absorbance spectra, retention times, accurate masses and MS/MS fragmentation patterns were compared with compounds from wildtype and mutant *A. thaliana* samples. Absorbance spectrum of compounds is given in the upper part; MS/MS fragmentation spectrum is provided in the lower part. *Numbers* correspond to spot numbers given in **a**

LC-PDA-QTOF-MS. These results indicate an in planta FLS activity of LDOX.

To analyse the effect of *FLS1* and/or *LDOX* knock-out in respect to possible feedback or feedforward regulation of genes in the flavonoid biosynthetic pathway, the expression of *CHS, F3H, FLS1, DFR*, *LDOX* and the two flavonoid/flavonol glycosyltransferase coding genes *UGT78D2* and *UGT89C1* was examined by RT-PCR in the respective mutant seedlings (Fig. 6b). No significant differences in expression were detected for genes encoding the upstream (Fig. 1) enzymes CHS and F3H and the downstream glycosyltransferase genes *UGT78D2* and *UGT89C1*. *DFR* and *LDOX* gene expression levels are lower in the Nö-0 accession than in the Col-0 accession, which is in accordance with the lower level of anthocyanins found in the Nö-0 wildtype. In the *fls1-2* mutant the *DFR* and *LDOX* expression is increased in comparison to the corresponding Nö-0 wildtype, fitting well to the enhanced accumulation of anthocyanin pigments observed in the *fls1-2* mutant. In contrast, *FLS1* expression is not increased in the *ldox* mutant. The missing *LDOX* expression seems to have no influence on the expression level of the analysed genes, while the *FLS1* knock-out influences the expression of the late flavonoid biosynthesis genes, but does not affect the expression of the early biosynthesis genes.

In situ flavonoid staining of mutant seedlings

The distribution of flavonol/dihydroflavonol accumulation in the various mutants and wildtype seedlings was visualized in planta with DPBA in norflurazon-bleached seedlings and imaged by epifluorescence microscopy. Representative pictures are shown in Fig. 7. As control the *chs* mutant was included which does not show any staining due to the absence of flavonoids. In the wildtypes, the cotyledons show intense orange fluorescence indicating massive accumulation of flavonols. Also the hypocotyl, the hypocotyl-root transition zone, root vascular tissue and the root tip display orange staining indicative of flavonols. No difference was observed between Col-0 and Nö-0. The *ldox* mutant seedling did not differ significantly from wildtype, except that the orange fluorescence seems to be more

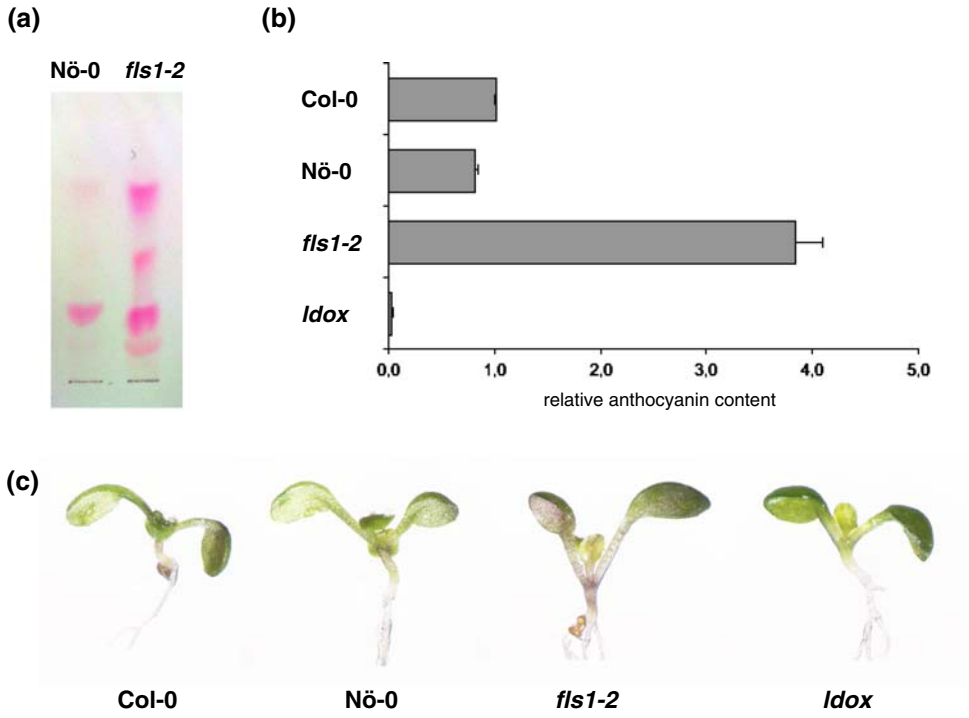

Fig. 5 Anthocyanin accumulation is increased in the *fls1-2* mutant. **a** HPTLC-separated anthocyanin derivatives. **b** Relative anthocyanin content of 5-day-old seedlings; referred to the amount in Col-0 seedlings. **c** Representative photographs of seedlings showing anthocyanin accumulation

Table 1 Differential metabolites in *fls1-2* seedlings identified by LC-PDA-QTOF-MS

RT (min)	Observed mass (*m/z*)	Calc. mass (*m/z*)	Δ Mass (ppm)	UV/Vis	MS fragments	Mol formula	Metabolite name (putative ID)	Nö-0 mean	Nö-0 SD	*fls1-2* mean	*fls1-2* SD	Ratio of *fls1-2*/Nö-0	*P*-value
12.54	627.1563	627.1556	1.17	286	465, 303	C27H30O17	Dihydroquercetin-dihexoside	9	0	1195	73	132.81	0.000010
12.74	465.1025	465.1038	−2.90	286	303	C21H22O12	Dihydroquercetin-hexoside 1	27	7	21953	865	823.23	0.000002
14.40	465.1040	465.1038	0.32	286	303	C21H22O12	Dihydroquercetin-hexoside 2	9	0	1785	218	198.37	0.000146
14.87	465.1038	465.1038	−0.11	286	303	C21H22O12	Dihydroquercetin-hexoside 3	9	0	1338	131	148.63	0.000062
15.28	595.1669	595.1668	0.09	278	449, 433	C27H32O15	Dihydrokaempferol-hexoside-deoxyhexoside 1	121	22	8881	583	73.60	0.000013
16.02	625.1793	625.1774	3.03	283	nd	C28H34O16	Methyl-dihydroquercetin-dihexoside 1	9	0	931	37	103.44	0.000002
16.31	449.1078	449.1089	−2.52	282	287	C21H22O11	Dihydrokaempferol-hexoside 1	67	5	7007	470	105.11	0.000014
16.96	479.1187	479.1184	0.63	286	317	C22H24O12	Methyl-dihydroquercetin-hexoside 1	9	0	5407	295	600.81	0.000006
17.22	611.1622	611.1618	0.73	nd	465, 303	C27H32O16	Dihydroquercetin-hexoside-deoxyhexoside 1	286	7	9877	777	34.50	0.000028
17.43	755.2062	755.2040	2.91	254, 354	609	C33H40O20	Quercetin-hexoside-dideoxyhexoside	26802	147	3513	251	0.13	0.000000
17.43				254, 354		C33H40O20	Quercetin-hexoside-dideoxyhexoside, isotope 1	10541	243	1228	74	0.12	0.000000
17.61	449.1104	449.1089	3.27	nd	nd	C21H22O11	Dihydrokaempferol-hexoside 2	84	2	2296	170	27.44	0.000023
18.14	449.1084	449.1089	−1.19	282	nd	C21H22O11	Dihydrokaempferol-hexoside 3	143	6	4144	431	28.98	0.000088
18.32	595.1659	595.1668	−1.59	286	nd	C27H32O15	Dihydrokaempferol-hexoside-deoxyhexoside 2	9	0	687	53	76.33	0.000024
18.64	465.1039	465.1038	0.11	nd	nd	C21H22O12	Dihydroquercetin-hexoside 4	9	0	1375	57	152.78	0.000002
19.00	739.2087	739.2091	−0.54	264, 348	593, 447	C33H40O19	Kaempferol-hexoside-dideoxyhexoside	29942	669	1217	31	0.04	0.000000
19.00				264, 348		C33H40O19	Kaempferol-hexoside-dideoxyhexoside, isotope 1	16582	2093	428	13	0.03	0.000003
19.00	625.1740	625.1774	−5.44	283	625	C28H34O16	Methyl-dihydroquercetin-dihexoside 2	56	12	958	36	17.11	0.000002
19.47	465.1044	465.1038	1.18	286	303	C21H22O12	Dihydroquercetin-hexoside 5	45	19	11908	5290	264.62	0.017771
19.62	958.2135	958.2148	−1.36	nd	931	C37H53O22NS3	Unknown 1	9	0	1375	1112	152.74	0.100619
19.65	593.1494	593.1512	−3.02	264, 324	nd	C27H30O15	Kaempferol-hexoside-deoxyhexoside 1	3304	461	102	25	0.03	0.000276
19.78	611.1606	611.1618	−1.89	283	465	C27H32O16	Dihydroquercetin-hexoside-deoxyhexoside 2	9	0	3232	854	359.07	0.002827
20.84	609.1472	609.1461	1.80	254, 353	463	C27H30O16	Quercetin-hexoside-deoxyhexoside	34216	110	9486	886	0.28	0.000001
20.84				254, 353		C27H30O16	Quercetin-hexoside-deoxyhexoside, isotope 1	19166	1758	2373	171	0.12	0.000002
21.17	449.1100	449.1089	2.37	278	303	C21H22O11	Dihydroquercetin-deoxyhexoside	9	0	28091	313	3121.22	0.000000
21.49	479.1210	479.1184	5.43	nd	nd	C22H24O12	Methyl-dihydroquercetin-hexoside 2	9	0	1993	103	221.41	0.000005
21.80	465.1032	465.1038	−1.40	286	303	C21H22O12	Dihydroquercetin-hexoside 6	32	4	21756	1054	672.87	0.000004
22.21	755.2023	755.2040	−2.27	nd	nd	C33H40O20	Unknown 2	1594	467	26	15	0.02	0.000114
23.26	593.1516	593.1512	0.67	264, 348	431	C27H30O15	Kaempferol-hexoside-deoxyhexoside 2	34383	4	7579	652	0.22	0.000000
23.26				264, 348		C27H30O15	Kaempferol-hexoside-deoxyhexoside 2, isotope 1	27215	3383	1989	162	0.07	0.000092
23.26				264, 348		C27H30O15	Kaempferol-hexoside-deoxyhexoside 2, isotope 2	3524	240	589	28	0.17	0.000005
23.55	593.1525	593.1512	2.19	254, 348	nd	C27H30O15	Quercetin-dideoxyhexoside	30487	118	5353	283	0.18	0.000000
23.55				254, 348	nd	C27H30O15	Quercetin-dideoxyhexoside, isotope 1	10607	238	1459	55	0.14	0.000000
23.55				254, 348	nd	C27H30O15	Quercetin-dideoxyhexoside, isotope 2	2012	51	675	23	0.34	0.000000
23.98	623.1597	623.1618	−3.30	254, 353	609	C28H32O16	Methyl-quercetin-hexoside-deoxyhexoside	28979	629	2672	314	0.09	0.000000

Table 1 continued

RT (min)	Observed mass (*m/z*)	Calc. mass (*m/z*)	Δ Mass (ppm)	UV/Vis	MS fragments	Mol formula	Metabolite name (putative ID)	Nö-0 mean	Nö-0 SD	*fls1-2* mean	*fls1-2* SD	Ratio of *fls1-2*/Nö-0	*P*-value
23.98				254, 353		C28H32O16	Methyl-quercetin-hexoside-deoxyhexoside, isotope 1	9322	475	781	99	0.08	0.000000
25.08	433.1159	433.1140	4.36	286	287	C21H22O10	Eriodictyol-deoxyhexoside	9	0	2934	245	326.00	0.000032
26.13	577.1543	577.1563	−3.42	264, 348	431	C27H30O14	Kaempferol-dideoxyhexoside	32814	450	3098	151	0.09	0.000000
26.13				264, 348		C27H30O14	Kaempferol-dideoxyhexoside, isotope 1	18287	2701	870	34	0.05	0.000009
26.13				264, 348		C27H30O14	Kaempferol-dideoxyhexoside, isotope 2	2530	282	215	15	0.09	0.000002
26.55	991.2314	991.2361	−4.75	nd	nd	C44H48O26	Unknown 3	9	0	1922	94	213.52	0.000004
26.91	607.1656	607.1668	−2.05	339	nd	C28H32O15	Methyl-quercetin-dideoxyhexoside	3057	101	370	6	0.12	0.000001
29.13	567.1346	567.1355	−1.66	nd	nd	C25H28O15	Unknown 4	98	20	3629	162	37.16	0.000003
32.27	591.1707	591.1719	−2.08	325	nd	C28H32O14	Methyl-kaempferol-dideoxyhexoside	2862	35	4071	47	1.42	0.000002
32.67	725.2075	725.2087	−1.66	288	nd	C36H38O16	Unknown 5	70	6	9	0	0.13	0.000061
36.11	1213.2883	1213.2948	−5.36	288	nd	C48H62O36	Unknown 6	89	8	662	23	7.44	0.000002

The software program *MetAlign* was used for unbiased mass peak extraction and alignment of data. Four thousand eight hundred and eighteen signals were clustered based on their retention time and corresponding behaviour over the samples as described by Tikunov et al. (2005), including natural isotopes, adducts and in-source fragments, derived from the same compound. Student's *t*-tests were performed to determine the significant differences between mutant and wildtype plants in the 221 obtained clusters and 292 single mass signals. Compounds were (putatively) identified by comparing several databases (see Sect. "Materials and methods"). Suggested elemental compositions and annotations were checked for the presence of corresponding in-source fragments in the mass clusters and for absorbance spectra in the original data files. In all cases of annotated flavonoids, the observed masses were within 5 ppm deviation from the calculated masses. A value of "9" corresponds to three times noise value, i.e. compound is below detection limit of the system

RT retention time (min); *observed mass* (*m/z*) averaged accurate mass ($[M\text{-}H]^-$), as mass-to-charge ratio; *calc mass* calculated accurate mass; *Δ mass* (ppm) deviation between the averages of observed and calculated accurate masses, in parts per million; *UV/Vis* absorbance maxima in the UV/Vis range (nd, not detectable absorbance); *MS fragments* MS fragments obtained through increased collision energy on indicated parent mass; *mol formula* molecular formula of the metabolite; *metabolite name* common name of putatively identified metabolite; *mean Nö-0/ mean fls1-2* data represent means from three separate experiments ±SD; *P-value* changes were compared by the Student's *t*-test

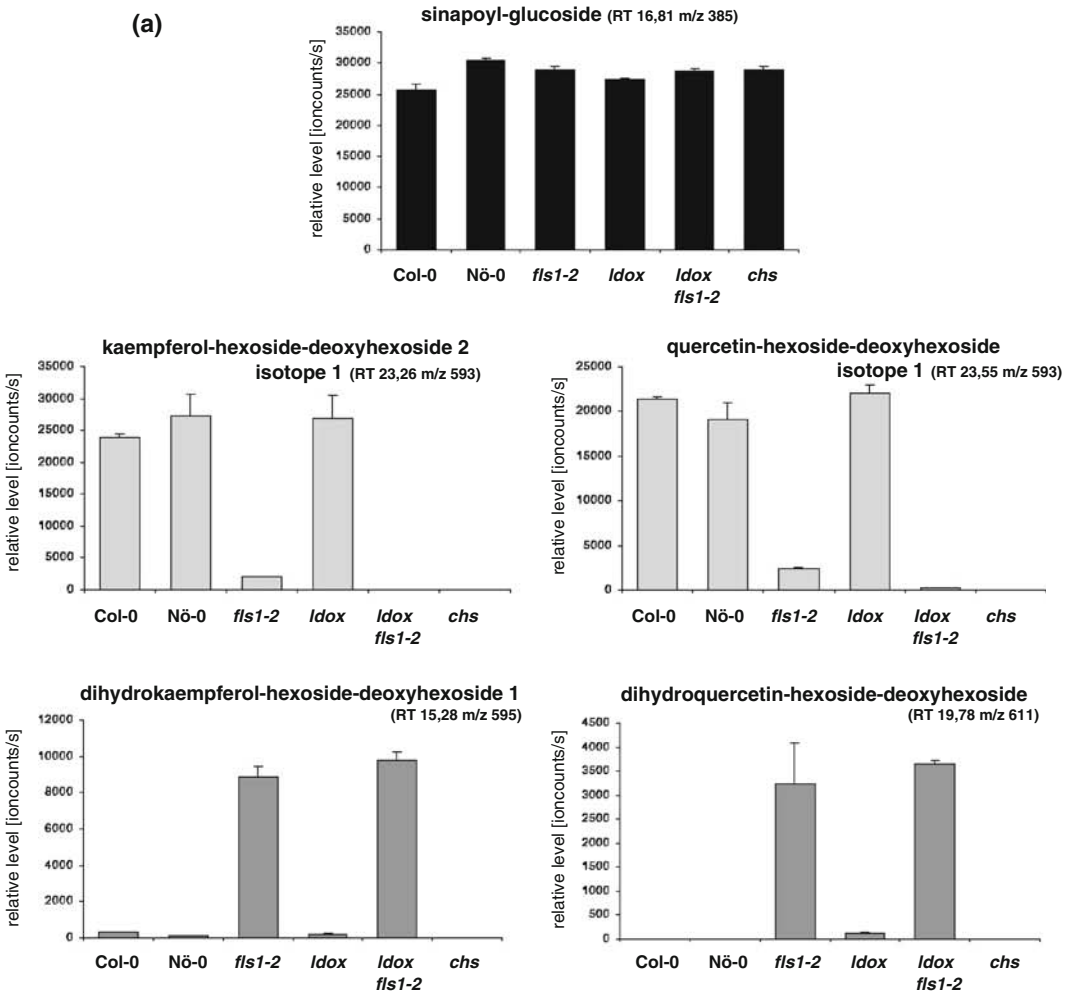
(a)
sinapoyl-glucoside (RT 16,81 m/z 385)
relative level [ioncounts/s]
Col-0
Nö-0
fls1-2
ldox
ldox fls1-2
chs
kaempferol-hexoside-deoxyhexoside 2 isotope 1 (RT 23,26 m/z 593)
quercetin-hexoside-deoxyhexoside isotope 1 (RT 23,55 m/z 593)
dihydrokaempferol-hexoside-deoxyhexoside 1 (RT 15,28 m/z 595)
dihydroquercetin-hexoside-deoxyhexoside (RT 19,78 m/z 611)

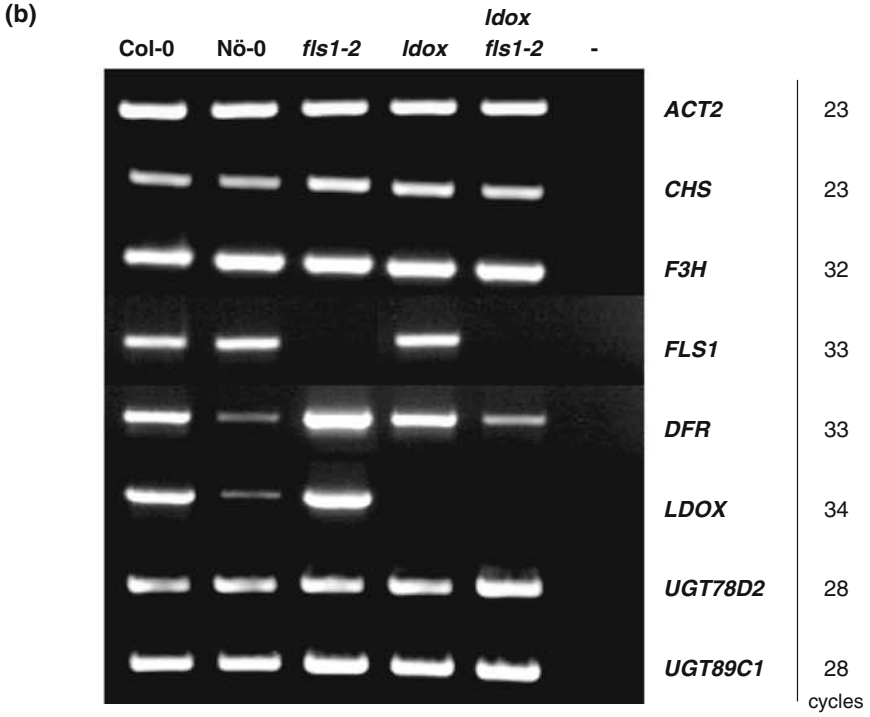
(b)
ldox
Col-0
Nö-0
fls1-2
ldox
fls1-2
-
ACT2 23
CHS 23
F3H 32
FLS1 33
DFR 33
LDOX 34
UGT78D2 28
UGT89C1 28
cycles

◀ **Fig. 6** Analysis of *ldox fls1-2* double mutant seedlings. **a** LC-PDA-QTOF-MS derived data showing relative amounts (ion counts per second, on top of the chromatographic peak) of selected flavonol glycosides and dihydroxyflavonol glycosides in seedlings of various mutants and wildtypes. Values for sinapoyl-glucoside are given as unaffected compound control. Compounds are putatively identified by their accurate mass ($[M-H]^-$), MS/MS fragments and PDA spectra. A clear reduction of flavonol glycoside accumulation is seen in the *ldox fls1-2* double mutant, compared to the *fls1-2* single mutant. There are still detectable very low amounts of flavonol glycosides in the *ldox fls1-2* mutant. Column height is not indicative between metabolites, since the MS detector response can differ markedly, even between very similar compounds. Signal intensities are linear in the range of about 200-25,000 ion counts s^{-1}. *Error bars* indicate standard error of means ($n = 3$). In cases were the detector was saturated from the monoisotopic parent, the first ^{13}C-isotope (isotope 1) intensities were used in the calculations. A table summarizing the LC-PDA-QTOF-MS derived data is presented as supplementary material (Supplementary Table 1). **b** Gene expression analysis of flavonoid biosynthesis genes in the *ldox fls1-2* mutant. Representative results from RT-PCR showing the accumulation of *ACT2, CHS, F3H, FLS1, DFR, LDOX, UGT78D2* and *UGT89C1* transcripts in 5-day-old *A. thaliana* wildtype and mutant seedlings. Numbers of amplification cycles are given at the *right*

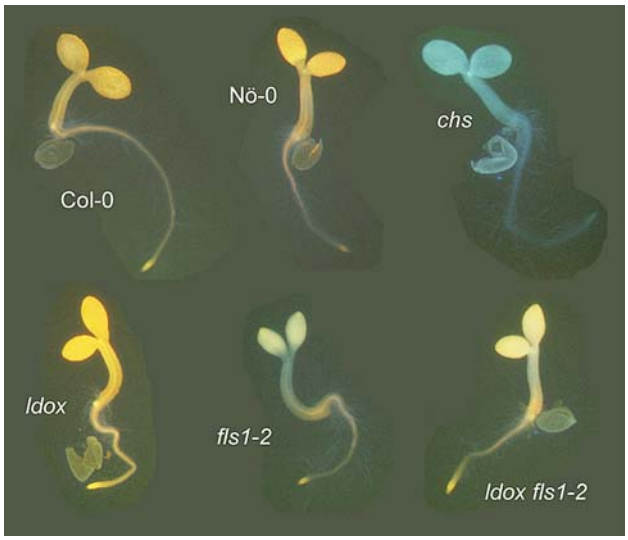

Fig. 7 In situ flavonol/dihydroflavonol staining of wildtype and mutant seedlings. Flavonols in intact, norflurazon-bleached seedlings were stained with DPBA until saturation and imaged by epifluorescence microscopy. Photographs of representative seedlings are shown

intensive, which could be indicative for enhanced flavonol accumulation, as also indicated by an enhanced quercetin-hexoside-deoxyhexoside level depending on a mutant *ldox* gene (Fig. 6a). *fls1-2* and *ldox fls1-2* seedlings essentially display a staining pattern similar to that of the wildtype. The observed staining in the *fls1-2* and *ldox fls1-2* mutant is less intensive in comparison to the wildtype, supposable due to different fluorescence intensities of DPBA-conjugates with flavonols and dihydroflavonols. Since the fluorescence in the wildtype seedlings could be traced back to flavonols, while in the *ldox fls1-2* seedling it could be almost exclusively attributed to dihydroflavonols (Fig. 6a), the in situ visualization showed, that distribution of dihydroflavonols in the *fls1-2* mutant seems to be unaltered from that of flavonols in the wildtype.

Discussion

Flavonol synthase was proposed to be the only enzyme activity of the central flavonoid biosynthesis pathway encoded by multiple loci in the *A. thaliana* genome (Pelletier et al. 1997; Wisman et al. 1998). The presence of multiple *FLS* genes in *A. thaliana* could allow differential expression and/or different substrate specificities of FLS isoforms. Beside the *FLS1* locus, five loci, designated *FLS2–FLS6*, show high similarity in the encoded deduced peptides. The clustered genomic arrangement of these genes (Fig. 2a), with a consecutive arrangement of *FLS2–FLS5*, suggests the formation from a common ancestor by gene duplication events. The duplications are likely to be ancient events, since some of the *FLS* genes seem to have lost their functionality after duplication. This notion is supported by a premature stop-codon in *FLS6*, an additional intron in *FLS4* causing a truncated protein and a missplicing of *FLS2* at the border of the second intron and the third exon, resulting in a frameshift and in a truncated protein version lacking key C-terminal residues required for 2-oxogluterate- and iron-binding. Thus, *FLS2, FLS4* and *FLS6* appear to be pseudogenes. However, *FLS3* and *FLS5* encode, like *FLS1*, full-length proteins and their transcripts were detected in developing seedlings (Fig. 2c).

The *fls2–fls6* single mutants did not show any obvious flavonol-related phenotype when analysed by HPTLC (Fig. 4a). In contrast, *fls1-2* mutant seedlings displayed a strong reduction of flavonol glycoside accumulation and a parallel accumulation of dihydroflavonol glycosides. Analyses of organs from adult *fls1-2* plants gave similar results as observed in seedlings (data not shown). Dihydroflavonols, aglycones and their glycosides, are widely distributed in ferns, gymnosperms and a variety of angiosperms (Iwashina 2003). Two dihydrokaempferol-hexosides were found in flesh of transgenic ripe tomato fruits overexpressing the maize transcription factors LC (BHLH) and C1 (R2R3-MYB) (Bovy et al. 2002; Le Gall et al. 2003). The accumulation of dihydroflavonol glycosides in the *fls1-2* mutant is remarkable, since, to our knowledge, these compounds have not been reported in *A. thaliana* plants before.

Dihydrokaempferol and dihydroquercetin are intermediates at a branching point of flavonoid biosynthesis, which are usually directly converted into anthocyanidins/proanthocyanidins (by the action of DFR) and/or flavonols (by the action of FLS). The increase of anthocyanin accumulation seen in the *fls1-2* mutant (Fig. 5) can to some extent be attributed to elevated expression of *DFR* and *LDOX* as

deduced from RT-PCR analyses (Fig. 6b). Dihydroflavonol precursors, usually channelled to flavonols, are converted by DFR to build anthocyanidins. A similar effect was observed previously by antisense expression of a petunia *FLS* cDNA in petunia and tobacco, which markedly reduced flavonol synthesis in petals and concurrently intensified red flower pigmentation (Holton et al. 1993). In the regulatory *A. thaliana* mutant *pfg1 pfg2 pfg3*, accumulation of flavonols is blocked while the accumulation of anthocyanins is increased (Stracke et al. 2007). This increase of anthocyanin accumulation is only possible in cells where in the wildtype plant *DFR* and *FLS1* are expressed simultaneously. We propose that cell types containing FLS1 but no DFR and LDOX activity in wildtype plants, accumulate dihydroflavonols in the *fls1-2* mutant which are subsequently stabilized and detoxified by glycosylation. This view is supported by the in situ DPBA staining pattern of bleached *ldox fls1-2* seedlings showing a distribution of dihydroflavonol glycosides resembling the occurrence of flavonols in wildtype (Fig. 7). On HPTLC plates, treatment of dihydroflavonols and dihydroflavonol glycosides with DPBA results in yellow/orange or green fluorescence colours (Fig. 4) similar to the ones described for quercetin and kaempferol aglycons and their 3- and/or 7-glycosides (Markham 1989; Sheahan and Rechnitz 1992). As a result, we were not able to clearly distinguish between flavonols and dihydroflavonols by in situ staining and the exact localization of flavonol glycoside compounds in *fls1-2* mutant plants could not be resolved. Assuming that the remaining flavonols in the *fls1-2* seedling are produced by a FLS side activity of the LDOX enzyme, we suggest that these compounds accumulate in cells expressing both *FLS1* and *LDOX* in the wildtype. The similar accumulation pattern of flavonols in the wildtype and dihydroflavonols in the *ldox fls1-2* mutant could imply that the glycosylation steps, leading to flavonol glycosides or dihydroflavonol glycosides, respectively, are performed by the same glycosyltransferases that are able to use both compounds as substrates (Fig. 1). In vitro studies of Jones et al. (2003) analyzing the substrate range of flavonoid glycosyltransferases showed that substrate recognition was broader than that predicted from a comparison of wildtype and knockout metabolite profiles. This is likely, given the very different contexts for enzyme action. In planta, the availability and concentration of substrates will influence product formation; as indicated by the occurrence of dihydroflavonol glycosides in the *fls1-2* mutant.

Another notable observation is the accumulation of an eriodictyol-deoxyhexoside in the *fls1-2* mutant, which is absent in the Nö-0 wildtype (Table 1). It is possible that the absence of FLS1 opens the way to the synthesis of eriodictyols from naringenin by flavonoid 3′-hydroxylase (F3′H) activity, as it has been shown that *A. thaliana* F3′H can convert naringenin into eriodictyol in vitro (Schoenbohm et al. 2000).

Our results from HPTLC metabolite analysis of *fls* mutants, together with the lacking activation of *FLS2–FLS6* promoters by PFG factors, indicate that the *FLS* genes *2-6* do not encode functional FLS and do not contribute to flavonol biosynthesis. During our study, Owens et al. (2008a) provided evidence for the same assumption. They followed a similar approach, using T-DNA insertion lines to explore the contributions of *FLS1–FLS6* genes to flavonoid biosynthesis. Only a *fls1* mutant (FLAG_55E06, Wassileskija accession, insertion in the 5′UTR that is different to the allele used in our study) exhibited a flavonoid-related phenotype with reduced kaempferol and quercetin levels and enhanced anthocyanidin accumulation. Furthermore, a lack of catalytical in vitro FLS activity of recombinant thioredoxin fusion proteins of FLS3 and FLS5 with dihydroflavonols and naringenin as substrates under a variety of conditions (variations in pH, temperature, enzyme and substrate concentrations, enzyme enrichment, cleavage procedures) was reported. Whether the *fls1* (FLAG_55E06) mutant does accumulate dihydroflavonol glycosides is not reported. The authors conclude that FLS1 appears to be the only member of the FLS family encoding a catalytically competent protein that influences flavonoid levels.

Like other dioxygenases, FLS contain several strictly conserved amino-acid residues (Lukacin and Britsch 1997) which include two histidines (His221, His277) and one acidic amino acid (223) residue for Fe^{II}-binding, an arginine (Arg287) together with a serine (Ser289) proposed to bind 2-oxoglutarate, and four amino acids (Gly68, His75, Gly261, Pro207) with no obvious functionality, presumed to be required for proper folding of the enzyme polypeptide (Wellmann et al. 2002). For FLS1 from *A. thaliana*, His132, Lys202 and Phe293 were identified via computational methods and analysed by mutational analyses in spectroscopic assays, showing their importance for dihydroquercetin substrate binding (Chua et al. 2008). Primary sequence comparison of *A. thaliana* FLS polypeptides sequences with other FLS proteins (Supplementary Figure 1) revealed some amino acid motifs, which are found in all FLS proteins but are absent from the FLS2–FLS6 polypeptides: (1) the amino acid motif PxxxIRxxxEQP at the N-terminus, (2) $CP^{Q}/_{R}PxLAL$ found upstream of the 2-oxoglutarate binding motif and (3) SxxTxLVP, located downstream of the second conserved region found in 2-oxoglutarate-dependent enzymes. These protein regions are potentially important for FLS activity, separating FLS from 2-oxoglutarate-/Fe^{II}-dependent dioxygenases with other substrate specificities. The importance of the PxxxIRxxxEQP motif at the N-terminus, that is missing in the FLS2–FLS6 polypeptides, was recently identified and further analysed by Owens et al. (2008a). In their study it

was shown that a N-terminal truncated FLS1 variant, lacking the first 21 N-terminal amino acids did not show in vitro FLS activity. The additional finding that the N-terminal region of FLS1 is not able to restore FLS activity to FLS5 in a chimeric protein shows that additional crucial amino acids are missing in FLS5, possibly within the two other motifs discussed above.

The observation that there are still small quantities of flavonol glycosides in the *fls1-2* null mutant led us to the generation of a *ldox fls1-2* double mutant. This was done under two assumptions: (1) that the *FLS2–FLS6* genes do not encode functional FLS and (2) that the LDOX enzyme could have FLS activity in vivo. The first assumption has been shown to be correct in this work and by the work of Owens et al. (2008a). The second assumption is based mainly on the work of Turnbull et al. (2003, 2004) and Yan et al. (2005). In vitro experiments with recombinant LDOX suggested that the enzyme could produce not only its natural product, cyanidin, but depending on the C-4 stereochemistry of the leucocyanidin substrate, possibly also dihydroquercetin and quercetin (Turnbull et al. 2003). Also, flavonols could be observed as a side product in *Escherichia coli* cells simultaneously expressing recombinant F3H, DFR, LDOX and a flavonoid 3-*O*-glucosyltransferase, potentially due to an alternate reaction catalysed by LDOX (Yan et al. 2005). The clear reduction of flavonol glycoside accumulation in the *ldox fls1-2* double mutant compared to the *fls1-2* single mutant (Fig. 6a) indicates that LDOX can indeed exert FLS activity in the seedling. Thus, this is the first direct evidence of in planta FLS activity of LDOX as suggested recently (Lillo et al. 2008; Owens et al. 2008a). The origin of the remaining very low amounts of flavonol glycosides in the *ldox fls1-2* mutant remains unclear and the physiological relevance of these traces (undetectable with HPTLC, PDA- and UV-detectors) is questionable. Although it appears that none of the other *A. thaliana FLS* genes can contribute FLS activity, it cannot be exclude that marginal FLS activity reside in the other FLS proteins analysed by in vitro assays (Owens et al. 2008a). A recent study reported in vivo FLS activity for FLS3 in a yeast biotransformation assay (A. Preuss and S. Martens, unpublished results). FLS3 is the closest homologue to FLS1 (Supplementary Figure 1), particularly in the regions of the iron- and 2-oxoglutarate binding motifs (A. Preuss and S. Martens, unpublished results). Besides this, it is also possible that another related two oxoglutarate dioxygenase can complement the lack of FLS1 (and LDOX). One candidate is F3H, which is thought to have overlapping in vivo activities with FLS1 and LDOX (Owens et al. 2008b). These proposals need further investigation.

Flavonoid biosynthetic genes are coordinately induced (Hahlbrock et al. 1976; Pelletier et al. 1999; Hartmann et al. 2005) and a sequential induction in the order of the biosynthetic steps in the flavonoid pathway has been suggested (Kubasek et al. 1992). This level of regulation may be to some extend achieved by feedforward or feedback mechanisms utilizing phenylpropanoid intermediates or end products, as shown for the enzyme L-phenylalanine ammonia lyase, whose activity is negatively regulated by its own product, *trans*-cinnamic acid (Bolwell et al. 1986; Blount et al. 2000) or for the bean *CHS* promoter, being regulated by the first two intermediates of the phenylpropanoid pathway, *trans*-cinnamic acid and *trans-p*-coumaric acid, in fungal elicitor treated alfalfa protoplasts (Loake et al. 1991). We analysed whether the expression of upstream, early enzyme genes (Fig. 1), such as *CHS* and *F3H*, and of downstream genes, like *UGT78D2* encoding a flavonoid 3-*O*-glucosyltransferase (Tohge et al. 2005) and *UGT89C1* coding for a flavonol 7-*O*-rhamnosyltransferase (Yonekura-Sakakibara et al. 2007), are affected by the loss of *FLS1/LDOX* and the accompanied lack or reduction of metabolites. The drastic reduction of flavonol glycosides and the lack of anthocyanins in the *ldox fls1-2* mutant have no detectable effect on the transcription of the early flavonoid biosynthesis genes *CHS* and *F3H*; therefore feedback regulation seems to be unlikely. Feedforward regulation also seems to be improbable, since the expression of the glycosyltransferase genes is not effected in the mutants. Suppression of *FLS1* expression, however, affects the expression of the late flavonoid biosynthesis genes *DFR* and *LDOX*, but does not affect the expression of the early biosynthesis genes. The *fls1-2* mutation does not change the flux to dihydroflavonols, but causes a metabolite flux into the competing anthocyanin branch pathway, leading to an enhanced accumulation of anthocyanins.

Similar rechannelling is known from other *A. thaliana* mutants defective in enzymes which are located at branching points of the flavonoid biosynthesis pathway, like the *dfr* mutant having increased total flavonol content in seeds (Routaboul et al. 2006) and the *banyuls* mutant showing abnormal anthocyanin accumulation in the seed due to a defect in ANR (Albert et al. 1997), and from the regulatory triple mutant *pfg1 pfg2 pfg3*, blocking the accumulation of flavonols while increasing the accumulation of anthocyanins (Stracke et al. 2007). However, the loss of *LDOX* seems neither to influence the expression of early nor of late biosynthesis genes, although a slight increase of flavonols is seen (Figs. 6a, 7). We conclude that, besides the described rechannelling effects, the total flux into flavonoids is supposably not changed in the *ldox fls1-2* mutant, since no effect on the expression of the early flavonoid biosynthesis genes could be observed.

Seedlings lacking the activity of the R2R3-MYB transcription factors PFG1–PFG3, are not able to accumulate flavonol glycosides (Stracke et al. 2007), indicating that the

formation of flavonol glycosides is exclusively dependent on these factors. Comparing the structural *fls1-2* mutant with the regulatory *pfg1 pfg2 pfg3* triple mutant, it is obvious that the lack of activation of *FLS1* by PFG factors is not sufficient to explain the absence of flavonol glycosides in the regulatory mutant. This leads to the assumption that (1) the block of flavonol glycoside production is due to a missing activation of genes downstream of *FLS1* in the flavonoid biosynthesis pathway. Candidates are the flavonol/dihydroflavonol glycosyltransferases, which were found to be activated by PFG factors (Stracke et al. 2007). (2) *LDOX* can be activated by PFG factors. Since it is widely accepted that late flavonoid biosynthesis genes are regulated by the combinatorial interaction of R2R3-MYB and BHLH factors (reviewed in Quattrocchio et al. 2006) and that the PFG R2R3-MYBs are flavonol-specific regulators (Mehrtens et al. 2005; Stracke et al. 2007), this second assumption seems to be unlikely, but certainly needs further investigation.

Initially, the working model for the experiments reported here was that FLS activity in *A. thaliana* might be encoded by more than one locus. The metabolic analysis of a *fls1-2* null mutant initially supported this model. Beside the unexpected accumulation of dihydroflavonol glycosides, *fls1-2* seedlings produced small quantities of flavonol glycosides, indicating the existence of non-FLS1 mediated in vivo FLS activity. This activity was, in contrast to our first hypothesis, not mediated by one or more of the *FLS* gene family members, but predominantly by a side activity of the LDOX enzyme in planta.

Acknowledgements We thank Melanie Kuhlmann for excellent technical assistance and the Sequencing Core Facility at the Bielefeld University for doing an excellent job in determining DNA sequences. This project was funded in part by the EU project FLAVO (FOOD-CT-2004-513960) and the GABI program of the Bundesministerium für Bildung und Forschung (BMBF)/Projektträger Jülich (PTJ).

References

Albert S, Delseny M, Devic M (1997) *BANYULS*, a novel negative regulator of flavonoid biosynthesis in the Arabidopsis seed coat. Plant J 11:289–299

Blount JW, Korth KL, Masoud SA, Rasmussen S, Lamb C, Dixon RA (2000) Altering expression of cinnamic acid 4-hydroxylase in transgenic plants provides evidence for a feedback loop at the entry point into the phenylpropanoid pathway. Plant Physiol 122:107–116

Bolwell GP, Cramer CL, Lamb CJ, Schuch W, Dixon RA (1986) l-Phenylalanine ammonia-lyase from *Phaseolus vulgaris*: modulation of the levels of active enzyme by trans-cinnamic acid. Planta 169:97–107

Bovy A, de Vos R, Kemper M, Schijlen E, Almenar Pertejo M, Muir S, Collins G, Robinson S, Verhoeyen M, Hughes S, Santos-Buelga C, van Tunen A (2002) High-flavonol tomatoes resulting from the heterologous expression of the maize transcription factor genes LC and C1. Plant Cell 14:2509–2526

Britsch L, Heller W, Grisebach H (1981) Conversion of flavanone to flavone, dihydroflavonol to flavonol with enzyme systems from cell cultures of parsley. Z Naturforsch C 36:742–750

Britsch L, Dedio J, Saedler H, Forkmann G (1993) Molecular characterization of flavanone 3 beta-hydroxylases. Consensus sequence, comparison with related enzymes and the role of conserved histidine residues. Eur J Biochem 217:745–754

Chenna R, Sugawara H, Koike T, Lopez R, Gibson TJ, Higgins DG, Thompson JD (2003) Multiple sequence alignment with the Clustal series of programs. Nucleic Acids Res 31:3497–3500

Chua CS, Biermann D, Goo KS, Sim TS (2008) Elucidation of active site residues of *Arabidopsis thaliana* flavonol synthase provides a molecular platform for engineering flavonols. Phytochemistry 69:66–75

Clifton IJ, McDonough MA, Ehrismann MD, Kershaw NJ, Granatino N, Schofield CJ (2006) Structural studies on 2-oxoglutarate oxygenases and related double-stranded β-helix fold proteins. J Inorg Biochem 100:644–669

De Vos RCH, Moco S, Lommen A, Keurentjes JJB, Bino RJ, Hall RD (2007) Untargeted large-scale plant metabolomics using liquid chromatography coupled to mass spectrometry. Nat Protoc 2:778–791

Edwards K, Johnstone C, Thompson C (1991) A simple and rapid method for the preparation of plant genomic DNA for PCR analysis. Nucleic Acids Res 19:1349

Forkmann G (1991) Flavonoids as flower pigments: the formation of the natural spectrum and its extension by genetic engineering. Plant Breed 106:1–26

Forkmann G, De Vlaming P, Spribille R, Wiering H, Schram AW (1986) Genetic and biochemical studies on the conversion of dihydroflavonols to flavonols in flowers of *Petunia hybrida*. Z Naturforsch C 41:179–186

Hahlbrock K, Knobloch KH, Kreuzaler F, Potts JR, Wellmann E (1976) Coordinated induction and subsequent activity changes of two groups of metabolically interrelated enzymes. Light-induced synthesis of flavonoid glycosides in cell suspension cultures of Petroselinum hortense. Eur J Biochem 61:199–206

Harborne JB, Williams CA (2000) Advances in flavonoid research since 1992. Phytochemistry 55:481–504

Hartmann U, Sagasser M, Mehrtens F, Stracke R, Weisshaar B (2005) Differential combinatorial interactions of cis-acting elements recognized by R2R3-MYB, BZIP, and BHLH factors control light-responsive and tissue-specific activation of phenylpropanoid biosynthesis genes. Plant Mol Biol 57:155–171

Heller W, Forkmann G (1994) Biosynthesis of flavonoids. In: Harborne JB (ed) The flavonoids. Chapman & Hall, London, pp 499–535

Holton TA, Brugliera F, Tanaka Y (1993) Cloning and expression of flavonol synthase from *Petunia hybrida*. Plant J 4:1003–1010

Iwashina T (2003) Flavonoid function and activity to plants and other organisms. Biol Sci Space 17:24–44

Jones P, Messner B, Nakajima J, Schaffner AR, Saito K (2003) UGT73C6 and UGT78D1, glycosyltransferases involved in flavonol glycoside biosynthesis in *Arabidopsis thaliana*. J Biol Chem 278:43910–43918

Keurentjes JJ, Fu J, De Vos RCH, Lommen A, Hall RD, Bino RJ, van der Plas LH, Jansen RC, Vreugdenhil D, Koornneef M (2006) The genetics of plant metabolism. Nat Genet 38:842–849

Kubasek WL, Shirley BW, McKillop A, Goodman HM, Briggs W, Ausubel FM (1992) Regulation of flavonoid biosynthetic genes in germinating Arabidopsis seedlings. Plant Cell 4:1229–1236

Le Gall G, DuPont MS, Mellon FA, Davis AL, Collins GJ, Verhoeyen ME, Colquhoun IJ (2003) Characterization and content of flavonoid glycosides in genetically modified tomato (*Lycopersicon esculentum*) fruits. J Agric Food Chem 51:2438–2446

Leonard E, Yan Y, Koffas MA (2006) Functional expression of a P450 flavonoid hydroxylase for the biosynthesis of plant-specific hydroxylated flavonols in *Escherichia coli*. Metab Eng 8:172–181

Lillo C, Lea US, Ruoff P (2008) Nutrient depletion as a key factor for manipulating gene expression and product formation in different branches of the flavonoid pathway. Plant Cell Environ 31:587–601

Loake GJ, Choudhary AD, Harrison MJ, Mavandad M, Lamb CJ, Dixon RJ (1991) Phenylpropanoid pathway intermediates regulate transient expression of a chalcone synthase gene promoter. Plant Cell 3:829–840

Lukacin R, Britsch L (1997) Identification of strictly conserved histidine and arginine residues as part of the active site in *Petunia hybrida* flavanone 3beta-hydroxylase. Eur J Biochem 249:748–757

Lukacin R, Wellmann F, Britsch L, Martens S, Matern U (2003) Flavonol synthase from *Citrus unshiu* is a bifunctional dioxygenase. Phytochemistry 62:287–292

Markham KR (1989) Flavones, flavonols and their glycosides. In: Dey PM, Harborne JB (eds) Methods in plant biochemistry. Academic Press, New York, pp 197–236

Martens S, Forkmann G (1999) Cloning and expression of flavone synthase II from Gerbera hybrids. Plant J 20:611–618

Martens S, Forkmann G, Matern U, Lukacin R (2001) Cloning of parsley flavone synthase I. Phytochemistry 58:43–46

Martens S, Forkmann G, Britsch L, Wellmann F, Matern U, Lukacin R (2003) Divergent evolution of flavonoid 2-oxoglutarate-dependent dioxygenases in parsley. FEBS Lett 544:93–98

Martin C, Prescott A, Mackay S, Bartlett J, Vrijlandt E (1991) Control of anthocyanin biosynthesis in flowers of *Antirrhinum majus*. Plant J 1:37–49

Mehrtens F, Kranz H, Bednarek P, Weisshaar B (2005) The Arabidopsis transcription factor MYB12 is a flavonol-specific regulator of phenylpropanoid biosynthesis. Plant Physiol 138:1083–1096

Moco S, Bino RJ, Vorst O, Verhoeven HA, de Groot J, van Beek TA, Vervoort J, de Vos CHR (2006) A liquid chromatography–mass spectrometry-based metabolome database for tomato. J Plant Physiol 141:1205–1218

Myllylä R, Günzler V, Kivirikko KI, Kaska DD (1992) Modification of vertebrate and algal prolyl 4-hydroxylases and vertebrate lysyl hydroxylase by diethyl pyrocarbonate. Evidence for histidine residues in the catalytic site of 2-oxoglutarate-coupled dioxygenases. Biochem J 286:923–927

Owens DK, Alerding AB, Crosby KC, Bandara AB, Westwood JH, Winkel BS (2008a) Functional analysis of a predicted flavonol synthase gene family in Arabidopsis. Plant Physiol 147:1046–1061

Owens DK, Crosby KC, Runac J, Howard BA, Winkel BS (2008b) Biochemical and genetic characterization of Arabidopsis flavanone 3beta-hydroxylase. Plant Physiol Biochem 46:833–843

Pelletier MK, Murrell JR, Shirley BW (1997) Characterization of flavonol synthase and leucoanthocyanidin dioxygenase genes in Arabidopsis. Plant Physiol 113:1437–1445

Pelletier MK, Burbulis IE, Shirley BW (1999) Disruption of specific flavonoid genes enhances the accumulation of flavonoid enzymes and endproducts in Arabidopsis seedlings. Plant Mol Biol 40:45–54

Prescott AG, Stamford NPJ, Wheeler G, Firmin JL (2002) In vitro properties of a recombinant flavonol synthase from *Arabidopsis thaliana*. Phytochemistry 60:589–593

Quattrocchio F, Wing JF, Leppen HTC, Mol JNM, Koes RE (1993) Regulatory genes controlling anthocyanin pigmentation are functionally conserved among plant species and have distinct sets of target genes. Plant Cell 5:1497–1512

Quattrocchio F, Baudry A, Lepiniec L, Grotewold E (2006) The regulation of flavonoid biosynthesis. In: Grotewold E (ed) The science of flavonoids. Springer, Columbus, pp 97–122

Reddy AM, Reddy VS, Scheffler BE, Wienand U, Reddy AR (2007) Novel transgenic rice overexpressing anthocyanidin synthase accumulates a mixture of flavonoids leading to an increased antioxidant potential. Metab Eng 9:95–111

Roach PL, Clifton IJ, Fulop V, Harlos K, Barton GJ, Hajdu J, Andersson I, Schofield CJ, Baldwin JE (1995) Crystal structure of isopenicillin N synthase is the first from a new structural family of enzymes. Nature 375:700–704

Ross JA, Kasum CM (2002) Dietary flavonoids: bioavailability, metabolic effects, and safety. Annu Rev Nutr 22:19–34

Routaboul JM, Kerhoas L, Debeaujon I, Pourcel L, Caboche M, Einhorn J, Lepiniec L (2006) Flavonoid diversity and biosynthesis in seed of *Arabidopsis thaliana*. Planta 224:96–107

Schoenbohm C, Martens S, Eder C, Forkmann G, Weisshaar B (2000) Identification of the *Arabidopsis thaliana* flavonoid 3′-hydroxylase gene and functional expression of the encoded P450 enzyme. Biol Chem 381:749–753

Sheahan JJ, Rechnitz GA (1992) Flavonoid-specific staining of *Arabidopsis thaliana*. Biotechniques 13:880–883

Sprenger-Haussels M, Weisshaar B (2000) Transactivation properties of parsley proline rich bZIP transcription factors. Plant J 22:1–8

Spribille R, Forkmann G (1984) Conversion of dihydroflavonols to flavonols with enzyme extracts from flower buds of *Matthiola incana* R. Br Z Naturforsch C 39:714–719

Stracke R, Ishihara H, Huep G, Barsch A, Mehrtens F, Niehaus K, Weisshaar B (2007) Differential regulation of closely related R2R3-MYB transcription factors controls flavonol accumulation in different parts of the *Arabidopsis thaliana* seedling. Plant J 50:660–677

Tikunov Y, Lommen A, de Vos CH, Verhoeven HA, Bino RJ, Hall RD, Bovy AG (2005) A novel approach for nontargeted data analysis for metabolomics. Large-scale profiling of tomato fruit volatiles. Plant Physiol 139:1125–1137

Tohge T, Nishiyama Y, Hirai MY, Yano M, Nakajima J, Awazuhara M, Inoue E, Takahashi H, Goodenowe DB, Kitayama M, Noji M, Yamazaki M, Saito K (2005) Functional genomics by integrated analysis of metabolome and transcriptome of Arabidopsis plants over-expressing an MYB transcription factor. Plant J 42:218–235

Turnbull JJ, Nagle MJ, Seibel JF, Welford RW, Grant GH, Schofield CJ (2003) The C-4 stereochemistry of leucocyanidin substrates for anthocyanidin synthase affects product selectivity. Bioorg Med Chem Lett 13:3853–3857

Turnbull JJ, Nakajima J, Welford RW, Yamazaki M, Saito K, Schofield CJ (2004) Mechanistic studies on three 2-oxoglutarate-dependent oxygenases of flavonoid biosynthesis: anthocyanidin synthase, flavonol synthase, and flavanone 3beta-hydroxylase. J Biol Chem 279:1206–1216

van Eldik GJ, Reijnen WH, Ruiter RI, van Herpen MMA, Schrauwen JAM, Wullems GJ (1997) Regulation of flavonol biosynthesis during anther and pistil development, and during pollen tube growth in *Solanum tuberosum*. Plant J 11:105–113

Welford RWD, Turnbull JJ, Claridge TDW, Prescott AG, Schofield CJ (2001) Evidence for oxidation at C-3 of the flavonoid C-ring during anthocyanin biosynthesis. Chem Commun 1828–1829

Wellmann F, Lukacin R, Moriguchi T, Britsch L, Schiltz E, Matern U (2002) Functional expression and mutational analysis of flavonol synthase from *Citrus unshiu*. Eur J Biochem 269:4134–4142

Winkel-Shirley B (2001) Flavonoid biosynthesis. A colorful model for genetics, biochemistry, cell biology, and biotechnology. Plant Physiol 126:485–493

Wisman E, Hartmann U, Sagasser M, Baumann E, Palme K, Hahlbrock K, Saedler H, Weisshaar B (1998) Knock-out mutants from an En-1 mutagenized *Arabidopsis thaliana* population generate new phenylpropanoid biosynthesis phenotypes. Proc Natl Acad Sci USA 95:12432–12437

Yan Y, Chemler J, Huang L, Martens S, Koffas MA (2005) Metabolic engineering of anthocyanin biosynthesis in *Escherichia coli*. Appl Environ Microbiol 71:3617–3623

Yonekura-Sakakibara K, Tohge T, Niida R, Saito K (2007) Identification of a flavonol 7-*O*-rhamnosyltransferase gene determining flavonoid pattern in Arabidopsis by transcriptome coexpression analysis and reverse genetics. J Biol Chem 282:14932–14941